

**INVESTIGATION OF TIME INTEGRATION SCHEMES
FOR FINITE ELEMENT ANALYSIS OF
METAL FORMING PROCESSES**

BY

RAMESHKUMAR SIVARAMAN

Bachelor of Technology

Indian Institute of Technology

Madras, India

1990

**Submitted to the Faculty of the
Graduate College of the
Oklahoma State University
in partial fulfillment of
the requirements for
the Degree of
MASTER OF SCIENCE
December, 1992**

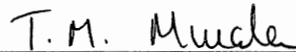
Thesis
1992
810242

INVESTIGATION OF TIME INTEGRATION SCHEMES
FOR FINITE ELEMENT ANALYSIS OF
METAL FORMING PROCESSES

Thesis Approved:



Thesis Adviser



Dean of the Graduate College

PREFACE

In the finite element simulation of metal forming processes the sources of errors that lead to volume change were studied. The study revealed that two major sources of error in volume change are the error in the velocity solution and the truncation error inherent in the updating scheme. Different methods for updating were implemented and simulation of experiments were carried out to compare with the experimental result. Effects of updating scheme on volume change and predicted loads were studied. The finite element formulation based on the penalty method leads to an excessive volume change if the penalty constant is not selected properly. A very large penalty constant leads to ill-condition of the stiffness matrix and the velocity solution does not converge. A simple method has been proposed to find an optimum value of the penalty constant that will ensure convergence of the velocity solution and effectively impose the incompressibility constraint.

The author wishes to express his deepest gratitude and sincere appreciation to his advisor, Dr. Yuh-Cheng Shiau for his exceptional guidance, encouragement and warm personal care throughout the present investigations. The author is also grateful to Dr. R. D. Delahoussaye and Dr. T. M. Minahen for reviewing the manuscript and for their helpful suggestions.

He also wishes to thank his parents for their endless encouragement, patience and support; and his colleagues and friends for their valuable discussions and their help in preparing the manuscript. Thanks are also due to Ms. Kalyani for her affection and understanding. Research support from National Center for Super Computing Applications is gratefully acknowledged.

TABLE OF CONTENTS

Chapter	Page
I. INTRODUCTION	1
II. FINITE ELEMENT APPROACH	4
Introduction	4
Basic Equations.....	5
Finite Element Discretization	8
Numerical Integration	9
III. THEORETICAL ANALYSIS	13
Review Of Time Integration Schemes.....	13
Numerical Methods and Error Analysis.....	15
Geometry Updating and Volume Loss.....	20
Plane-Strain Case	21
Axisymmetric Case	24
Example.....	26
Penalty Method	31
Introduction.....	31
Penalty Constant	33
Condition Number.....	38
Example.....	40
Conclusions	42
IV. RESULTS AND DISCUSSION.....	43
Introduction	43
Simulation Results.....	47
V. CONCLUSIONS AND RECOMMENDATIONS	59

Chapter	Page
REFERENCES.....	61
APPENDICES.....	63
APPENDIX A - ROUTINES FOR VOLUME CALCULATION FOR AXISYMMETRIC UNIFORM DEFORMATION PROCESS USING EULER FORWARD METHOD AND TRAPEZOIDAL METHOD.....	64
APPENDIX B - ROUTINES FOR VOLUME CALCULATION FOR AXISYMMETRIC UNIFORM DEFORMATION PROCESS USING AM-2 METHOD.....	66

LIST OF FIGURES

Figure	Page
3.1 Two-Dimensional Uniform Deformation of a Rectangular Element.....	22
3.2 Axisymmetric Uniform Deformation of a Rectangular Element	24
3.3 Volume Loss with Reduction in Height for Euler Forward Method	28
3.4 Volume Loss with Reduction in Height for the Trapezoidal Method.....	29
3.5 Volume Loss with Reduction in Height for AM-2 Method.....	30
3.6 Volumetric Strain-Rate vs Penalty Constant at Time $t = 0$	33
3.7 Volume Loss with Deformation for Different Values of Penalty Constant	37
3.8 Condition Number of the Stiffness Matrix vs Penalty Constant.....	40
3.9 Condition Number vs Tolerance.....	41
4.1 Block Diagram for Simulation Using Euler Forward Method	45
4.2 Block Diagram for Simulation Using the Trapezoidal Method.....	46
4.3 Illustration of the Quarter Taken for Simulation [56 Nodes and 42 Elements].....	48
4.4 Initial Mesh Used in FE Analysis of Cylinder Upsetting.....	48
4.5 Load vs Displacement for Friction Factor of $m = 0.0$	50
4.6 Volume Loss vs Height Reduction (%) for Friction Factor $m = 0.0$	51
4.7 Load vs Displacement for Friction Factor of $m = 0.25$	52
4.8 Volume Loss vs Height Reduction (%) for Friction Factor $m = 0.25$	53
4.9 Load vs Displacement for Friction Factor of $m = 1.0$	54
4.10 Volume Loss vs Height Reduction (%) for Friction Factor $m = 1.0$	55

Figure	Page
4.11 Volume Loss with Stroke (mm) Using ALPID 2.0.....	56
4.12 Load vs Stroke Using ALPID 2.0.....	57
4.13 Measured Microhardness Contours, ALPID Predictions with Single Internal-State-Variable Model (Upper Right Quadrant) and ALPID Predictions Using the Trapezoidal Method for Updating Microhardness (Lower Right Quadrant) for Height Reduction of 14.48 mm at 255°C.....	58

LIST OF TABLES

Table	Page
2.1 Integration Points and Weighting Factors of the Gaussian Quadrature Formula	12
3.1 Error Formulas for Plane-Strain Case	23
3.2 Error Formulas for Axisymmetric Case	26
3.3 Numerical Value of c for Different Values of Penalty Constant	36

NOMENCLATURE

FEM	Finite Element Method
AM-2	Adams-Moulton two-step
Δt	time increment
h	step size
$h\tau(h)$	local truncation error
Y_k	true solution at the k^{th} step
y_k	numerical solution at the k^{th} step
$Y^{(n)}(\xi)$	n th derivative at ξ
K	penalty constant
c	constant for the norm difference between the true and numerical solution using the penalty method
m	friction factor
$\ v\ _2$	Euclidean norm of vector v
(ξ, η)	natural coordinates
(x, y)	global coordinates
J	Jacobian matrix of coordinate transformation
σ	stress tensor
ϵ	strain tensor

CHAPTER I

INTRODUCTION

The finite element method (FEM) provides an efficient tool for proper design and control of forming processes. For proper design and control the knowledge of detailed deformation mechanics and an accurate prediction of the forming load, as well as the distribution of stress, strain, and strain-rate are important. The rigid-viscoplastic material model based on the penalty constant approach is used for FEM simulation. This has been incorporated in a finite element based software ALPID (Analysis of Large Plastic Incremental Deformation) for two dimensional model [ALPID 2D, 1987] and three dimensional simulation model [ALPID 3D, 1987].

The formulation based on penalty constant approach gives excessive volume change if the value of the penalty constant is not selected properly. Maintaining the volume change within a small percentage of the total deforming volume is a serious consideration in the prediction of proper die filling, which is important in process design. The volume change occurs because of the numerical approximations used in finding the velocity solution and updating the geometry. To effectively control the volume change, error in the velocity solution and the error in updating the geometry should be compatible. In other words there is no advantage in reducing one of the errors far below the other because the larger one will dominate.

Euler forward method, a first-order method, is commonly used [Kobayashi et al., 1989] for updating state variables. In this method the current step geometry is based on the geometry and velocity at the previous step and the time increment. In the finite element simulation of a typical forging process with constant die-velocity, the previous step

generally has less nodal velocities and strain-rates than the current step. Hence Euler forward method always underpredicts values at the current step, which leads to significant volume loss and underpredicted load values. An extensive study was carried out to select an appropriate updating scheme to overcome the drawbacks present in the Euler forward method. Both explicit and implicit methods [Osakada and Nakano, 1982] [Atkinson, 1989] [Hoff and Taylor, 1990] were examined for their suitability and ease of implementation on FEM programs.

The trapezoidal method and the Adams-Moulton 2-step (AM-2) method were selected to study their effect on volume change and predicted loads. The volume change during the compression of a simple 2-D element assuming constant rate of deformation was calculated. In this calculation the effects of friction and strain-hardening were neglected. Under ideal conditions both the trapezoidal and AM-2 methods are better than Euler forward method with respect to volume loss. The finite element based code SPID (Simple Plastic Incremental Deformation) by Kobayashi et al. [1989] was modified to implement the trapezoidal and AM-2 methods. Simulation of the cylinder upsetting experiments [Lee and Altan, 1972] was performed using SPID and its modified versions. The results obtained are better than those predicted by ALPID [Rusia and Gunasekara, 1989]. It is also observed that there is no significant difference in the results obtained between the trapezoidal and AM-2 methods. Simulation of the experiments by Lalli [1988] using the modified ALPID was carried out. In this simulation microhardness was updated using the trapezoidal method.

Influence of various factors on the error in the velocity solution was studied. It was observed that the volumetric strain-rate is inversely proportional to the penalty constant [Oden, 1981] [FIDAP, 1991]. Theoretically the error in the velocity solution can be reduced to any desired level by choosing a large penalty constant. However, with a very large penalty constant the velocity solution fails to converge because the stiffness matrix becomes ill-conditioned. Moreover, after a certain level, increasing the penalty constant

can not reduce volume change further because the truncation error inherent in the updating scheme dominates. The machine precision and the error tolerance specified have a very strong influence on K . The effect of tolerance on the convergence of the velocity solution was also studied. It was found that the condition number of the stiffness matrix increases with K . Hence, it is necessary to find an 'optimum' value for the penalty constant to impose the constraint of volume constancy and to ensure convergence of the velocity solution. A simple method is proposed for estimating the 'optimum' value of K , which can effectively impose the incompressibility condition as well as ensure convergence of the velocity solution.

CHAPTER II

FINITE ELEMENT APPROACH

Introduction

Several methods of deformation analysis of metals have been developed, with various degrees of approximations and idealizations. The finite element method seems to be the most powerful tool for analyzing metal forming processes because of its flexibility, adaptability, and accuracy. In this chapter the finite element formulation required for deformation analysis is presented in brief. Heat transfer analysis should also be carried out for hot forming processes. The elasto-viscoplastic flow model and the rigid viscoplastic flow model are the two most popular models used in the FE simulation of metal forming processes.

For plastic or viscoplastic materials in large deformation processes, elastic deformation can be considered to be negligible. The constitutive relations can be expressed [Zienkiewicz and Godbole, 1974] in an Eulerian form linking the stresses and current strain-rates. This is identical to the flow of viscous, non-Newtonian incompressible fluid because viscosity depends on the current strain-rates. The constitutive relation for a viscous, incompressible fluid is

$$\dot{\epsilon}_{ij} = \frac{1}{2\mu} \sigma'_{ij} \quad (2.1)$$

where σ'_{ij} are the deviatoric components of stress and the scalar μ is the viscosity which can be a function of strain, strain-rate, and temperature. Metals have a well-defined plastic yield stress and μ is given by

$$\mu = \frac{\bar{\sigma} + \gamma \dot{\epsilon}^p}{3 \dot{\epsilon}} \quad (2.2)$$

where $p < 1$, and $\bar{\sigma}$, the effective stress, is a function of $\bar{\epsilon}$, $\dot{\epsilon}$ and T . $\gamma = 0$ for ideal plastic metals and hence μ is given by

$$\mu = \frac{\bar{\sigma}}{3 \dot{\epsilon}} \quad (2.3)$$

Therefore Eqn. (2.1) becomes

$$\dot{\epsilon}_{ij} = \frac{3}{2} \frac{\dot{\epsilon}}{\bar{\sigma}} \sigma'_{ij} \quad (2.4)$$

A detailed discussion of these equations are given in the sections to follow. The constitutive relation represented by Eqn. (2.4) is identical to the isotropic elastic relations for incompressible solids with strain-rates taking place of strains. Thus all methods in solid mechanics developed for incompressible elastic materials can be used for viscous flow problems. This can be done provided displacements are interpreted as velocities and strains (infinitesimal) as strain-rates.

Basic Equations

The theory of plasticity deals with the time independent behavior of material adequately, but not with the time-dependent behavior. For the analysis of time-dependent

behavior of material in moderate range of temperatures, the theory of plasticity is generalized to cases which include strain-rate sensitivity. Assuming isotropy, negligible elastic deformation and Huber-Mises yield criterion, the constitutive relation can be expressed as

$$\dot{\epsilon} = \frac{3}{2} \frac{\dot{\bar{\epsilon}}}{\bar{\sigma}} \sigma' \quad (2.5)$$

where σ' and $\dot{\epsilon}$ are the deviatoric stress tensor and the strain-rate tensor, respectively. The effective stress $\bar{\sigma}$ and effective strain-rate $\dot{\bar{\epsilon}}$ are defined as

$$\bar{\sigma} = \left(\frac{3}{2} \sigma'^T \sigma' \right)^{1/2} \quad (2.6)$$

$$\dot{\bar{\epsilon}} = \left(\frac{2}{3} \dot{\epsilon}^T \dot{\epsilon} \right)^{1/2} \quad (2.7)$$

The effective stress (flow stress) for a specific material is determined by uniaxial tension or compression tests as a function of strain, strain-rate, and temperature as

$$\bar{\sigma} = \bar{\sigma}(\bar{\epsilon}, \dot{\bar{\epsilon}}, T) \quad (2.8)$$

The deformation of a rigid-viscoplastic material obeying the constitutive relation, Eqn. (2.5), is associated with many boundary value problems e.g. forging, extrusion, rolling etc.

A body of volume V is considered with traction f^* prescribed on a part of the surface S_F and velocity v^* prescribed on the remainder of the surface S_V . The deformation process is assumed as a static problem by neglecting the inertia effect and body force. The stress σ and velocity field v satisfy the following relations.

(1) equilibrium equations;

$$\nabla \cdot \boldsymbol{\sigma} = 0 \quad (2.9)$$

(2) constitutive equations;

$$\dot{\boldsymbol{\varepsilon}} = \frac{3}{2} \boldsymbol{\sigma}' \dot{\lambda} = \frac{3}{2} \frac{\dot{\boldsymbol{\varepsilon}}}{\boldsymbol{\sigma}} \boldsymbol{\sigma}' \quad (2.10a)$$

$$\text{and} \quad \bar{\boldsymbol{\sigma}} = \bar{\boldsymbol{\sigma}}(\bar{\boldsymbol{\varepsilon}}, \dot{\boldsymbol{\varepsilon}}, T) \quad (2.10b)$$

(3) incompressibility condition;

$$\dot{\boldsymbol{\varepsilon}}_v = \nabla \cdot \mathbf{v} = 0 \quad (2.11)$$

(4) strain-rate velocity relations;

$$\dot{\boldsymbol{\varepsilon}} = \frac{1}{2} (\nabla \mathbf{v} + (\nabla \mathbf{v})^T) \quad (2.12)$$

(5) boundary conditions;

$$\boldsymbol{\sigma} \mathbf{n} = \mathbf{f}^* \text{ on } S_F \quad (2.13a)$$

$$\mathbf{v} = \mathbf{v}^* \text{ on } S_v \quad (2.13b)$$

where $\dot{\boldsymbol{\varepsilon}}_v$ is the volumetric strain-rate, and \mathbf{n} is the unit vector normal to the corresponding surface.

Thus the unknowns for the solution of a quasi-static plastic deformation process are six stress components, six strain-rate components, and three velocity components. The governing equations are three equilibrium equations, six strain-rate velocity relations, and

six constitutive equations derived from the associated flow rule. The boundary conditions are prescribed in terms of velocity and traction [Kobayashi et al., 1989].

Since it is not possible to obtain an analytical, i.e., closed form solution, various approximate methods are used. Using the variational approach or the weighted residual method a simplified form can be obtained.

$$\int_V \sigma^T \delta \dot{\epsilon} dV - \int_{S_F} \mathbf{f} \delta \mathbf{v} dS = 0 \quad (2.14a)$$

To obtain the weak form, the integrand of the first term is replaced with the deviatoric stress and the hydrostatic pressure, and the hydrostatic part with a large positive penalty function K in order to satisfy the incompressibility condition. Then the following is obtained

$$\int_V \sigma'^T \delta \dot{\epsilon} dV + K \int_V \dot{\epsilon}_v \delta \dot{\epsilon}_v dV - \int_{S_F} \mathbf{f} \delta \mathbf{v} dS = 0 \quad (2.14b)$$

Finite Element Discretization

The weak form, Eqn. (2.14b), originated from the equilibrium equations associated with rigid-viscoplastic materials, is valid not only over the entire volume but also for any portion of the volume. If volume V is divided into M elements interconnected at N nodal points, then Eqn. (2.14) can be written at the element level as

$$\sum_e \left(\int_{V^{(e)}} \sigma'^T \delta \dot{\epsilon} dV + K \int_{V^{(e)}} \dot{\epsilon}_v \delta \dot{\epsilon}_v dV - \int_{S_F^{(e)}} \mathbf{f} \delta \mathbf{v} dS \right) = 0 \quad (2.15)$$

where e represents summation over all the elements.

Inside each element, the velocity distribution is approximated by a linear combination of certain interpolation functions with the nodal velocities at the element nodes. A linear function is used mostly because it yields a simple derivation to formulate the stiffness matrix and a lower degree of integration scheme (number of integration points) can be used. For higher accuracy and flexibility in the element deformation, higher order interpolation functions are used. A comprehensive discussion can be found in Ravi [1992].

For 2-D analysis with 4-node quadrilateral elements, the volume integral for the first term in Eqn. (2.15) was evaluated using 2×2 integration points whereas 1×1 integration points was used for the second term. The line integral, i.e., the third term in Eqn. (2.15), was carried out using 1 integration point.

Nonlinear solvers are used to obtain the velocity solution. Once the velocity solution is obtained the deformed geometry of the workpiece can be obtained by updating nodal coordinates. Currently Euler forward method is used as the updating scheme. There is a significant volume loss during the time increment after the geometry is updated.

Numerical Integration

All volume and surface integrations are performed by applying Gaussian quadrature formulas. As an example calculation of the deforming volume is presented in this section. Elemental volumes were calculated by numerical integration. These were then added to obtain the total volume. The formulas used in 2-D analysis for volume calculations are as follows :

For plane-strain deformation

$$A = \sum_e \left(\int \int dA \right) = \sum_e \left(\int \int |J| d\xi d\eta \right) \quad (2.16)$$

For axisymmetric deformation

$$V = \sum_e \left(\int \int \int dV \right) = 2\pi \sum_e \left(\int \int |J| r d\xi d\eta \right) \quad (2.17)$$

where $|J|$ is the determinant of the Jacobian matrix of coordinate transformation, and (ξ, η) is the natural coordinate system. The transformation from the natural (ξ, η) to the global coordinate (x, y) is

$$\mathbf{J} = \begin{bmatrix} \frac{\partial x}{\partial \xi} & \frac{\partial y}{\partial \xi} \\ \frac{\partial x}{\partial \eta} & \frac{\partial y}{\partial \eta} \end{bmatrix} \quad (2.18)$$

and

$$|J| = \frac{\partial x}{\partial \xi} \frac{\partial y}{\partial \eta} - \frac{\partial y}{\partial \xi} \frac{\partial x}{\partial \eta}$$

For isoparametric quadrilateral element with a bilinear shape function the elements of the Jacobian matrix is given as follows.

$$\frac{\partial x}{\partial \xi} = \sum_{\alpha} \frac{1}{4} (1+\xi_{\alpha}) (1+\eta_{\alpha}\eta) x_{\alpha} \quad \frac{\partial y}{\partial \xi} = \sum_{\alpha} \frac{1}{4} (1+\xi_{\alpha}) (1+\eta_{\alpha}\eta) y_{\alpha} \quad (2.19a)$$

$$\frac{\partial x}{\partial \eta} = \sum_{\alpha} \frac{1}{4} (1+\xi_{\alpha}\xi) (1+\eta_{\alpha}) x_{\alpha} \quad \frac{\partial y}{\partial \eta} = \sum_{\alpha} \frac{1}{4} (1+\xi_{\alpha}\xi) (1+\eta_{\alpha}) y_{\alpha} \quad (2.19b)$$

where (x_{α}, y_{α}) are the coordinates associated with the α th node.

Since the derivatives of the shape functions are linear in ξ and η , $|J|$ is a bilinear function in ξ and η . In other words $|J|$ is a combination of $\xi\eta$, ξ , η , and 1. Similarly, $r|J|$ is a quadratic function with combination of $\xi^2\eta$, $\xi\eta^2$, $\xi\eta$, ξ , η , and 1. Thus for plane-strain deformation, exact integration can be carried over a minimum of 1×1 integration point(s) whereas for axisymmetric deformation 2×2 integration points is required. In this study 2×2 integration points were used for volume calculation as the cylinder upsetting experiment was treated as a 2-D axisymmetric problem.

Applying the Gaussian quadrature formula we have the finite element formulation for 2-D axisymmetric case is obtained in the following form.

$$V = 2\pi \sum_e \left(\sum_{J=1}^2 \sum_{I=1}^2 r(\xi_I, \eta_I) |J(\xi, \eta)| W_I W_J \right) \quad (2.20)$$

where ξ_I and η_I are integration points and W_I are weighting factors. Integration points and associated weighting factors are listed in Table 2.1 [Kobayashi et al., 1989].

TABLE 2.1
 INTEGRATION POINTS AND WEIGHTING FACTORS OF
 THE GAUSSIAN QUADRATURE FORMULA

n	x_I	W_I
1	0	2.0
2	$\pm 0.577\ 350\ 269$	1.0
3	$\pm 0.774\ 596\ 669$ 0.000 000 000	0.555 555 556 0.888 888 889
4	$\pm 0.861\ 136\ 312$ $\pm 0.339\ 981\ 044$	0.347 854 845 0.652 145 155

n = number of integration points

x_I = coordinate of integration points

W_I = integration weighting factors

CHAPTER III

THEORETICAL ANALYSIS

Review of Time Integration Schemes

Extensive study was carried out to select a suitable time marching scheme that can be used for updating state variables in FE simulation of metal forming processes. Various textbooks were referred for standard numerical methods and research papers were studied to look for the latest developments in this area. Selecting an appropriate method requires the following aspects be taken into account [Hoff and Taylor, 1989].

1. The discretized partial differential equation has a truncation error composed of time and spatial approximation. In many cases the accuracy of spatial discretizations are no more than second order in space. Thus a higher order time step scheme will increase the cost without changing the spatial error. The objective in using higher order methods is to minimize the additional effort. In the current study the total error is composed of the error in velocity solution and in updating. Choice of a higher order method will reduce the error in updating. But this will lead to a better result only if velocity solution is of the same order or higher order accuracy than updating.
2. Higher order multistep methods need special starting procedures. The accuracy is maintained only when the higher derivatives of the right hand side function fulfill some continuity requirements. Hence proper care must be taken for application in problems where discontinuities occur, e.g., plasticity, fracture mechanics, and contact problems. These may not be useful for non-linear dynamic problems which require stringent

stability criteria. In this study the trapezoidal method was used to start the solution procedure for AM-2 method.

3. Function evaluations (calculation of velocities, forces etc.) are the most expensive part in non-linear problems which are discretized. Thus the required number of function evaluations reflects the usefulness of an algorithm. The utility of higher order extrapolation method requires large numbers of function evaluations to maintain accuracy especially when discontinuities occur. In the penalty constant approach the error in velocity solution can be reduced to any level by using a large penalty constant. If choice of a higher order method is made for updating, then the error in the velocity solution will have to be decreased. This decrease should be such that the error in the velocity is compatible with the truncation error of the updating method. To decrease the error in the velocity solution, a larger penalty constant must be used along with a smaller tolerance on the velocity solution. This will require more number of iterations for nonlinear solvers and thereby more time to obtain the velocity solution.

The general algorithm for single step time marching [Zienkiewicz et al, 1984] is a series of general algorithms of order p . It not only covers most of the currently used schemes but also presents many new possibilities. This is suitable for use in dynamic or diffusion equations. It is easy to program in its universal form for all orders of approximation. It is computationally advantageous in many cases over the conventional procedures especially the Newmark algorithm [Bathe, 1982] and its variants. However, this algorithm requires higher derivatives and hence does not qualify for use in the current study.

Investigation of higher order derivative, explicit one step methods by Hoff and Taylor [1990] showed that it is suitable for arbitrary non-linear analysis of structural dynamic problems. Their algorithm has acceleration at the current step as the primary unknown. Hence this method also cannot be used.

The Beta-m method as a generalization of the Newmark scheme by Katona and Zienkiewicz [1985] unifies the old and new methods and is computationally efficient. This method is not suitable in its general form for the current study because it requires acceleration at the current and previous step. In its simplest form it is Euler forward method, which is already in use.

The variable-order variable-step algorithms for second order systems [Thomas and Gladwell, 1990] can be used with local error estimators based on embedding techniques. In one of its simplest forms it yields the trapezoidal method. The advantages offered by this method in its general form requires acceleration. Hence, this method cannot be used in the current study.

Among higher order methods, the trapezoidal method and Adams-Moulton methods [Atkinson, 1989] can be used in this study. The order of these methods is higher than Euler forward method. Use of velocities from multiple steps, p , can be made to achieve a higher order of accuracy. But this will not be reflected in the result (volume change) after a certain increase in p because the error in velocity, which cannot be reduced after a certain level, will dominate. Hence only the trapezoidal method and Adams-Moulton 2-step method will be studied in greater detail and later implemented on FEM source codes. Their effect on the phenomenon of volume change and underpredicted loads will be analyzed. It will also be studied to ascertain their suitability in updating other state variables.

Numerical Methods and Error Analysis

Preliminary analysis of both explicit and implicit numerical methods, which are used in time integration, was carried out. In this section three numerical methods for solving initial value problems, namely, Euler forward method, the trapezoidal method, and Adams-Moulton 2-step method (AM-2 method) are discussed. The last two are implicit, higher order methods.

Consider the following differential equation :

$$Y'(t) = f(t, Y(t)) \quad \text{over } [x_n, x_{n+1}] \quad (3.1)$$

Integration of Eqn. (3.1) yields

$$Y_{n+1} = Y_n + \int_{x_n}^{x_{n+1}} f(t, Y(t)) dt \quad (3.2)$$

where Y_{n+1} denotes the true solution at x_{n+1} .

Theoretically all the three methods can be derived from Eqn. (3.2) using interpolation polynomials in the following form

$$Y_{n+1} = Y_n + \int_{x_n}^{x_{n+1}} Y'(t) dt = Y_n + \int_{x_n}^{x_{n+1}} [P_p(t) + E_p(t)] dt \quad (3.3)$$

where $P_p(t)$ denotes a polynomial of degree $\leq p$ that interpolates $Y'(t)$ at $x_{n+\delta-p}, \dots, x_{n+\delta}$, with $\delta = 0$ for explicit methods and $\delta = 1$ for implicit methods; and $E_p(t)$ is the error formula of the interpolating polynomial [Atkinson, 1989]. $P_p(t)$ can be conveniently written in the form of Lagrange multiplier functions $L_i(t)$ as

$$P_p(t) = \sum_{i=0}^p L_i(t) Y'(x_{n+\delta-i}) \quad (3.4)$$

where

$$L_i(t) = \prod_{j \neq i} \left(\frac{t - x_{n+\delta-j}}{x_{n+\delta-i} - x_{n+\delta-j}} \right) \quad i = 0, 1, \dots, p \quad (3.5)$$

$E_p(t)$ can be expressed as

$$E_p(t) = \frac{(t - x_{n+\delta-p}) \cdots (t - x_{n+\delta})}{(p+1)!} Y^{(p+2)}(\xi) \quad x_{n+\delta-p} \leq \xi \leq x_{n+\delta} \quad (3.6)$$

Eqn. (3.3) becomes

$$Y_{n+1} = Y_n + \int_{x_n}^{x_{n+1}} \sum_{i=0}^p L_i(t) Y'(x_{n+\delta-i}) dt + \int_{x_n}^{x_{n+1}} E_p(t) dt \quad (3.7)$$

Using different values of p in Eqn. (3.7), one can derive all the three numerical methods along with the associated truncation error. To derive the local truncation error, it is assumed that there is no difference between the numerical and true solutions at steps prior to $n+1$, i.e. $y_i = Y_i$ and $y'_i = Y'_i$, $i = n+\delta-p, \dots, n$. With $p=0$ and $\delta = 0$, integration of Eqn. (3.7) yields

$$Y_{n+1} = Y_n + hY'_n + \frac{h^2}{2} Y''(\xi) \quad (3.8)$$

where $x_n \leq \xi \leq x_{n+1}$ and $h = x_{n+1} - x_n$ is the step size.

By dropping the error term, $\frac{h^2}{2} Y''(\xi)$, often called the truncation error or the discretization error [Atkinson,1989] at x_{n+1} , the formula for Euler forward method is obtained in the following form.

$$y_{n+1} = y_n + hy'_n \quad (3.9)$$

where y_{n+1} denotes the numerical solution at x_{n+1} . With $y_n = Y_n$ and $y'_n = Y'_n$ the local truncation error $h\tau(h)$ is

$$h\tau(h) = Y_{n+1} - y_{n+1} = \frac{h^2}{2} Y''(\xi) \quad (3.10)$$

Substituting $\delta = 1$ and $p=1$ in Eqn. (3.7), i.e. interpolating $Y'(t)$ at the 2 points, x_{n+1} and x_n , the trapezoidal method can be derived as

$$Y_{n+1} = Y_n + \frac{h}{2} [Y'_n + Y'_{n+1}] - \frac{h^3}{12} Y^{(3)}(\xi) \quad (3.11)$$

Neglecting the error term yields the trapezoidal method in the following form

$$y_{n+1} = y_n + \frac{h}{2} [y'_n + y'_{n+1}] \quad (3.12)$$

The local truncation error $h\tau(h)$ is written as

$$h\tau(h) = Y_{n+1} - y_{n+1} = \frac{h}{2} [Y'_{n+1} - y'_{n+1}] - \frac{h^3}{12} Y^{(3)}(\xi) \quad (3.13)$$

$$|h\tau(h)| = |Y_{n+1} - y_{n+1}| \leq L |Y_{n+1} - y_{n+1}| + \left| \frac{h^3}{12} Y^{(3)}(\xi) \right| \quad (3.14)$$

where L is given as

$$L = \frac{h}{2} \frac{[Y'_{n+1} - y'_{n+1}]}{Y_{n+1} - y_{n+1}} = \frac{h}{2} \frac{\partial f(\eta)}{\partial y} \quad (3.15)$$

Lipschitz condition requires that $\partial f(\eta)/\partial y$ is a finite value, i.e. $L = O(h) \ll 1$. It will be seen later in this chapter that Lipschitz condition is satisfied by the state variable being updated. If the Lipschitz condition is satisfied then the following approximation can be made without any significant loss in accuracy.

$$h\tau(h) \cong -\frac{h^3}{12} Y^{(3)}(\xi) \quad (3.16)$$

Adams-Moulton methods are the most widely used multistep methods. They are used to produce predictor-corrector algorithms in which the error is controlled by varying both step size h and order of the method. To derive AM-2 method the integral formula, Eqn. (3.7), is used again but now, $Y'(t) = f(t, Y(t))$ is interpolated at the three points, x_{n+1} , x_n and, x_{n-1} . Substituting $p=2$ and $\delta = 1$ in Eqn. (3.7) and integrating it yields

$$Y_{n+1} = Y_n + \frac{h}{12} [5 Y'_{n+1} + 8 Y'_n - Y'_{n-1}] - \frac{h^4}{24} Y^{(4)}(\xi) \quad (3.17)$$

Dropping the error term leads to the numerical method associated with AM-2 method in the form given below.

$$y_{n+1} = y_n + \frac{h}{12} [5 y'_{n+1} + 8 y'_n - y'_{n-1}] \quad (3.18)$$

The local truncation error $h\tau(h)$ is given as

$$|h\tau(h)| = |Y_{n+1} - y_{n+1}| \leq L |Y_{n+1} - y_{n+1}| + \left| \frac{h^4}{24} Y^{(4)}(\xi) \right| \quad (3.19)$$

where L is given by

$$L = \frac{5h}{12} \frac{[Y'_{n+1} - y'_{n+1}]}{Y_{n+1} - y_{n+1}} \quad (3.20)$$

With Lipschitz condition, $L = O(h) \ll 1$, the local truncation error is

$$h\tau(h) \cong -\frac{h^4}{24} Y^{(4)}(\xi) \quad (3.21)$$

Euler forward method is an explicit method as y_{n+1} doesn't depend on itself. However, the trapezoidal method and AM-2 method represented by Eqn. (3.12) and Eqn. (3.18), respectively, are implicit methods as y_{n+1} appears as an argument on the right-hand side. The local truncation error for Euler forward method is of order $O(h^2)$, for the trapezoidal method it is of order $O(h^3)$, and for AM-2 method it is of order $O(h^4)$. Thus, it can be concluded that as far as local truncation error is concerned AM-2 method and the trapezoidal method are superior to Euler forward method. Both Euler forward method and the trapezoidal method are single step methods whereas AM-2 method is a multiple step method. Multiple step methods require a special starting procedure. In this study the trapezoidal method was used to start the solution procedure for AM-2 method.

Geometry Updating and Volume Loss

Volume change during compression of a simple axisymmetric 2-D element assuming uniform deformation was calculated. In the analysis of uniform deformation processes, effects of friction and strain-hardening are completely neglected. Error formulas were derived based on the local truncation error to estimate the total volume change after a certain amount of reduction. Volume change was calculated after updating the geometry using all the three methods. These were compared with the volume change calculated using error formulas. All the required data was generated using computer programs with floating point numbers of 64 bits. It can be seen from Eqn. (3.12) and Eqn. (3.18) that y_{n+1} depends on itself. Hence both the implicit methods are nonlinear with root y_{n+1} . The simple direct iteration method, the most convenient method for solving for nonlinear roots, was used to find the solution. Previous step solution y_n was taken as an initial guess of the solution y_{n+1} . To avoid any possible scaling effects fraction norm was calculated as

$$\left| \frac{y_{n+1}^{(j)} - y_{n+1}^{(j+1)}}{y_{n+1}^{(j+1)}} \right| \leq \epsilon \quad (3.22)$$

where the superscript denotes the iteration number and $\epsilon = 10^{-8}$ is the tolerance specified. A maximum of 7 iterations was required to achieve an accuracy of eight decimal digits in the solution. Thus, in the current study simple direct iteration method turned out to be convenient and quite efficient too. As an example the calculations discussed above was performed for the axisymmetric case. Extension to the plane-strain case is straightforward. Pertinent equations for both cases are given in the following sections.

Plane-Strain Case

There is a change in volume of elements after the geometry is updated with time increment Δt . Consider the two-dimensional plane-strain uniform deformation of a rectangular element, as shown in Fig. 3.1, where the element (1234) with a width of W_0 and a height of H_0 is deformed to the shape (12'3'4') with a width W_1 and height H_1 after a time increment Δt .

The volume constancy requires [Kobayashi, 1989] that

$$V = WH = \text{const.} \quad (3.23)$$

where V is the volume of the element. Differentiating Eqn. (3.23) with respect to time gives

$$\frac{\dot{W}}{W} = -\frac{\dot{H}}{H} \quad (3.24)$$

Repeating differentiation of Eqn. (3.24) with respect to time yields

$$W^{(2)} = 2W \left(\frac{\dot{H}}{H}\right)^2; \quad W^{(3)} = -6W \left(\frac{\dot{H}}{H}\right)^3; \quad W^{(4)} = 24W \left(\frac{\dot{H}}{H}\right)^4 \quad (3.25)$$

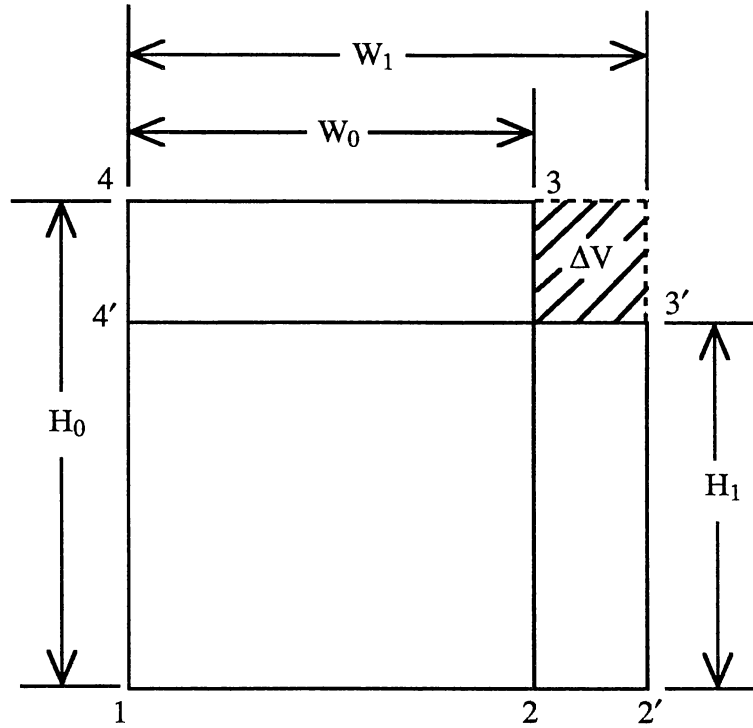


Figure 3.1 Two-Dimensional Uniform Deformation of a Rectangular Element

The change in height after a time increment Δt is given by

$$\Delta H_1 = \Delta t \dot{H}_0 = H_1 - H_0 = h_1 - H_0 \quad (3.26)$$

There is no error involved in updating the coordinate H using any of the methods because the velocity remains constant i.e. $\dot{H}_0 = \dot{H}_1 = \text{const.}$, during a uniform deformation process.

After a time Δt , the volume change can be calculated using

$$\frac{\Delta V_1}{V} = \frac{w_1 h_1 - W_1 H_1}{W_1 H_1} \cong -\frac{\Delta t \tau(\Delta t)}{W_1} \quad (3.27)$$

where w_1 and h_1 represent numerical solutions of width and height, respectively and ΔV_1 is the amount of volume change during the time increment Δt . Eqn. (3.27) can be simplified and is presented in Table 3.1.

Thus there is a volume loss during a time increment when geometry is updated by Euler forward method, which is indicated by the negative sign on $\Delta V_1/V$. But there is a gain in volume when using AM-2 method as indicated by the positive sign on $\Delta V_1/V$. For the trapezoidal method the sign on volume change is governed by the sign of ΔH . The volume loss rate is proportional to $\left(\frac{\Delta H}{H}\right)^2$ for Euler forward method, $\left(\frac{\Delta H}{H}\right)^3$ for the trapezoidal method, and $\left(\frac{\Delta H}{H}\right)^4$ for AM-2 method.

TABLE 3.1
ERROR FORMULAS FOR PLAIN-STRAIN CASE

	Euler forward method	trapezoidal method	AM-2 method
$w_1 =$	$W_0 + \Delta t \dot{w}_0$	$W_0 + \frac{\Delta t}{2} (\dot{w}_0 + \dot{w}_1)$	$W_0 + \frac{\Delta t}{12} (5 \dot{w}_0 + 8 \dot{w}_1 - \dot{w}_{-1})$
$W_1 - w_1 \cong$ $\Delta t \tau(\Delta t) \cong$	$\frac{(\Delta t)^2}{2} W^{(2)}(\xi)$	$-\frac{(\Delta t)^3}{12} W^{(3)}(\xi)$	$-\frac{(\Delta t)^4}{24} W^{(4)}(\xi)$
$\frac{\Delta V_1}{V} \cong$	$-\left(\frac{\Delta H}{H_0}\right)^2$	$-\frac{1}{2} \left(\frac{\Delta H}{H_0}\right)^3$	$\left(\frac{\Delta H}{H_0}\right)^4$

Axisymmetric Case

Consider the axisymmetric uniform deformation of a rectangular element, as shown in Fig. 3.2 where the element (1234) with a radius of R_0 and a height of H_0 is deformed to the shape (12'3'4') with a radius R_1 and height H_1 after a time increment Δt . In this case volume constancy requires

$$V = \pi R^2 H = \text{const.} \quad (3.28)$$

where R and H is the radius and height of the element, respectively, and V is the volume.

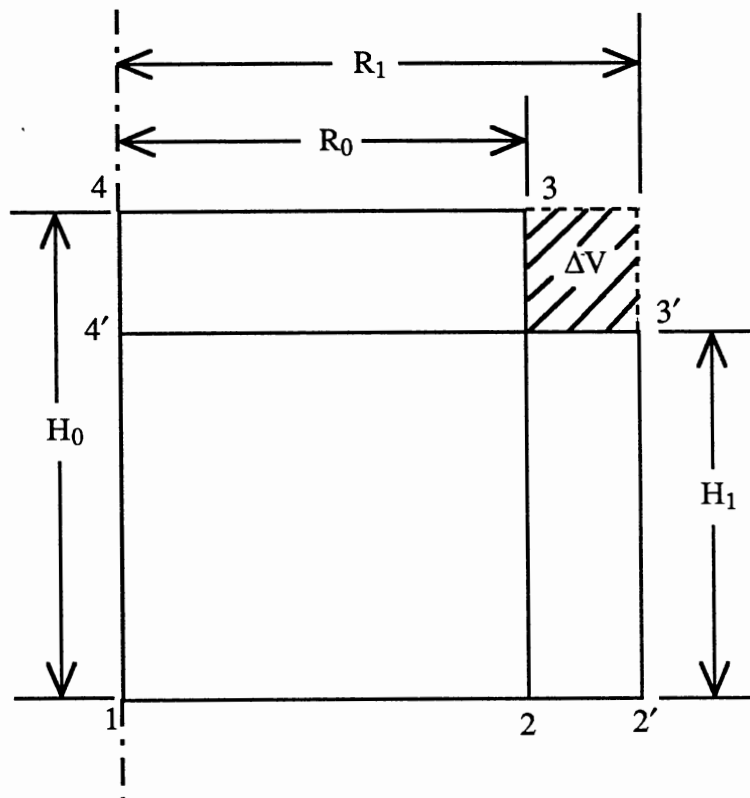


Figure 3.2 Axisymmetric Uniform Deformation of a Rectangular Element

Differentiating Eqn. (3.28) with respect to time gives

$$\frac{2\dot{R}}{R} = -\frac{\dot{H}}{H} \quad (3.29)$$

where dot represents time derivative and $\dot{H} = \dot{H}_0 = \text{const.}$, since velocity remains constant during uniform deformation. Repeating differentiation of Eqn. (3.29) with respect to time yields

$$R^{(2)} = \frac{3}{4} R \left(\frac{\dot{H}}{H}\right)^2; \quad R^{(3)} = -\frac{15}{8} R \left(\frac{\dot{H}}{H}\right)^3; \quad R^{(4)} = \frac{105}{16} R \left(\frac{\dot{H}}{H}\right)^4 \quad (3.30)$$

After a time Δt , volume change can be calculated using

$$\Delta V_1 = \pi (r_1^2 h_1 - R_1^2 H_1) \quad (3.31)$$

where r_1 and h_1 are the numerical solutions of radius and height, respectively.

Once again since uniform deformation is considered there is no error in updating the coordinate H irrespective of the method selected for updating. Since $h_1 = H_1$, Eqn. (3.31) can be further simplified, using the relation $r_1 = R_1 - \Delta t \tau(\Delta t)$ and neglecting the higher order terms, as

$$\frac{\Delta V_1}{V} \cong \frac{-2\pi\Delta t \tau(\Delta t)R_1H_1}{\pi R_1^2 H_1} = -\frac{2\Delta t \tau(\Delta t)}{R_1} \quad (3.32)$$

Eqn. (3.32) can be simplified for different methods and is listed in Table 3.2.

Table 3.2 shows that volume is lost after updating for Euler forward method whereas there is a gain in volume for AM-2 method. Once again for the trapezoidal method this depends on ΔH . Comparison of volume loss formulas for axisymmetric deformation

with those of plane-strain deformation shows that, the volume loss rate is of the same order for a given method irrespective of the type of uniform deformation.

TABLE 3.2
ERROR FORMULAS FOR AXISYMMETRIC CASE

	Euler forward method	trapezoidal method	AM-2 method
$r_1 =$	$R_0 + \Delta t \dot{r}_0$	$R_0 + \frac{\Delta t}{2} (\dot{r}_0 + \dot{r}_1)$	$R_0 + \frac{\Delta t}{12} (5 \dot{r}_1 + 8 \dot{r}_0 - \dot{r}_{-1})$
$R_1 - r_1 \cong$ $\Delta t \tau(\Delta t) \cong$	$\frac{(\Delta t)^2}{2} R^{(2)}(\xi)$	$-\frac{(\Delta t)^3}{12} R^{(3)}(\xi)$	$-\frac{(\Delta t)^4}{24} R^{(4)}(\xi)$
$\frac{\Delta V_1}{V} \cong$	$-\frac{3}{4} \left(\frac{\Delta H}{H_0}\right)^2$	$-\frac{5}{16} \left(\frac{\Delta H}{H_0}\right)^3$	$\frac{35}{64} \left(\frac{\Delta H}{H_0}\right)^4$

Example

The results obtained from compression of a simple axisymmetric 2-D element assuming uniform deformation is presented in this section. The total volume loss at any step is found by subtracting the current volume from the initial volume. The estimated

incremental volume loss was also calculated at every step. This was done using the error estimation formulas listed in Table 3.2.

The initial height and radius is 1m and the velocity is 1m/s, $\dot{H}_0 = \dot{H} = -1.0$ m/s. Time increments of 0.01 and 0.05 were used. The numerical values of L is calculated as follows :

For the trapezoidal method

$$L = \frac{\Delta t}{2} \frac{\partial \dot{R}_i}{\partial R_i} \leq \left| -\frac{\Delta t}{4} \frac{\dot{H}}{H_i} \right|_{\max} = 0.0125 \ll 1 \quad (3.33)$$

For AM-2 method

$$L = \frac{5 \Delta t}{12} \frac{\partial \dot{R}_i}{\partial R_i} \leq \left| -\frac{5 \Delta t}{24} \frac{\dot{H}}{H_i} \right|_{\max} = 0.014 \ll 1 \quad (3.34)$$

where subscript i represents the step number.

Thus the use of error formulas is justified because the Lipschitz condition is satisfied by both the trapezoidal and AM-2 methods and there is no precondition required for Euler forward method. The total estimated volume change at any step is found by summing the estimated incremental volume change. The total volume change as a function of deformation for step sizes of $\Delta H/H_0$ of 0.01 and 0.05 is plotted in Figs. 3.3, 3.4, and 3.5 for Euler forward method, the trapezoidal method, and AM-2 method, respectively. It is observed that estimated volume change using error formulas from Table 3.2 compares well with the actual volume change found by updating the geometry for all three methods. Hence it can be concluded that, preliminary analysis can be carried out using error estimation formulas which require less computational effort and time.

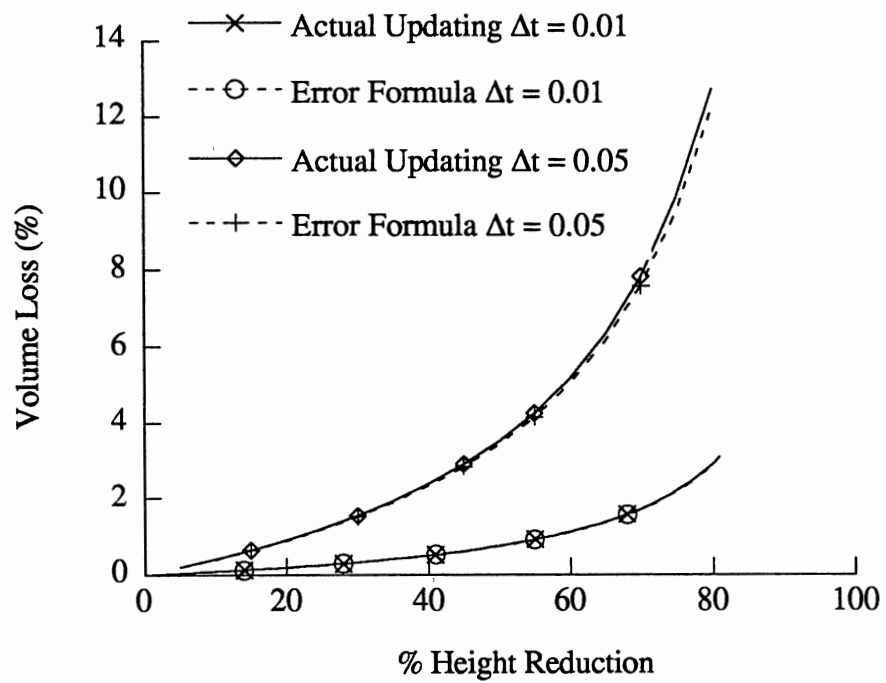


Figure 3.3 Volume Loss with Reduction in Height for Euler Forward Method

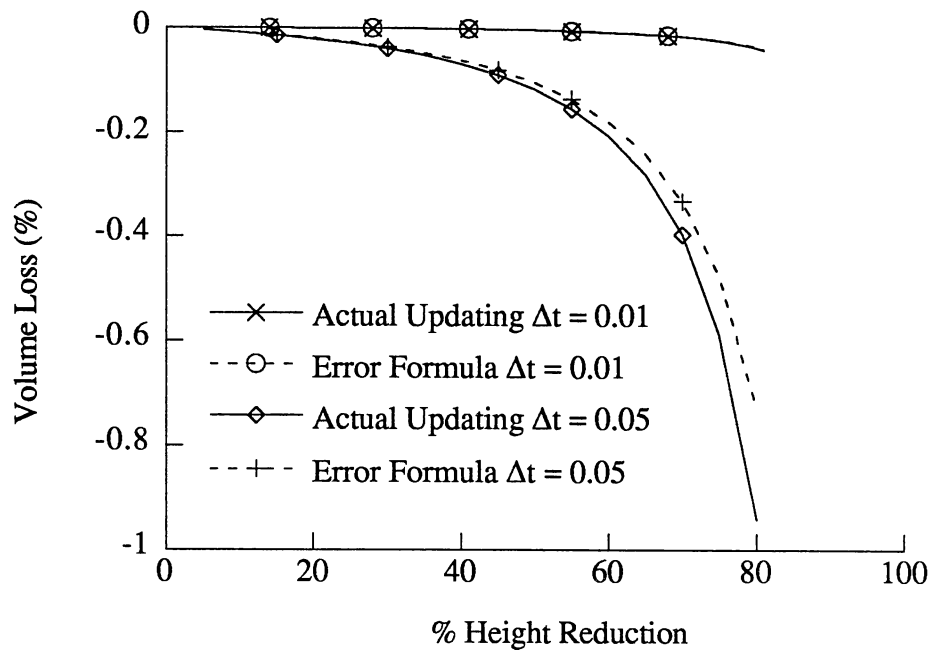


Figure 3.4 Volume Loss with Reduction in Height for the Trapezoidal Method

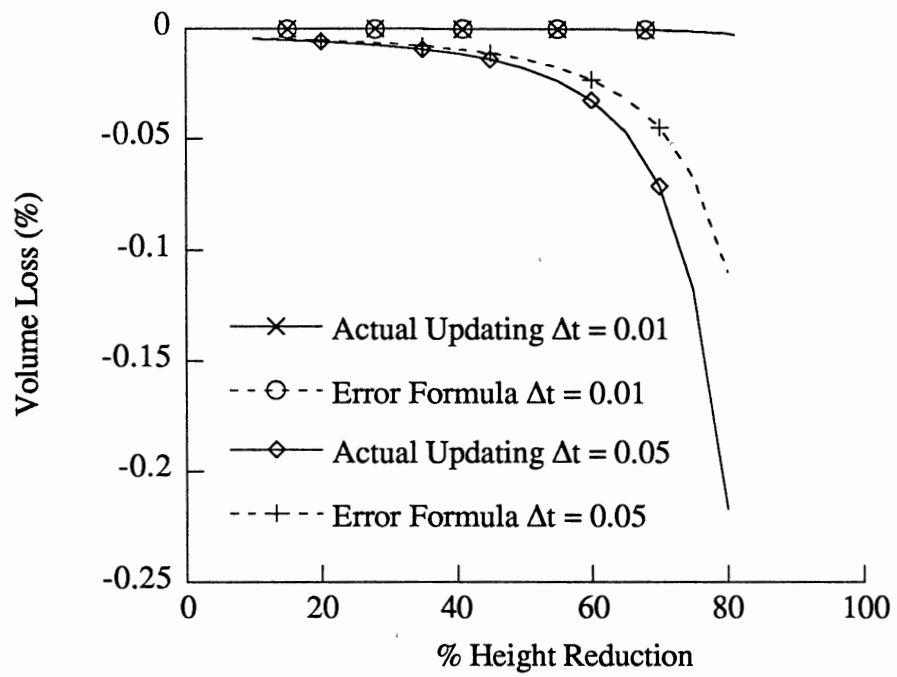


Figure 3.5 Volume Loss with Reduction in Height for AM-2 Method

Thus for updating geometry, AM-2 method results in the least volume change. It is also observed that the trapezoidal method is superior to Euler forward method with respect to volume change. In short both the higher order methods can be used in time integration schemes to give better results than Euler forward method.

Euler forward method has already been implemented in many of the FEM codes currently available, e.g., SPID, ALPID 2.0 etc. Both the aforementioned higher order methods will be implemented on SPID. The trapezoidal method requires the current and previous step velocities whereas AM-2 method additionally requires the velocity of the step before the previous step. Hence AM-2 method needs special starting procedure. As will be seen later, predicted forming load compares better with experimental data when strain is updated from the strain-rate solution using the trapezoidal method or AM-2 method.

Penalty Method

Introduction

Mathematically the penalty formulation can be equated to simulating the flow of a very slightly compressible fluid [FIDAP, 1986]. Since the governing differential equation cannot be solved analytically, numerical methods like FEM are used. Theoretically the velocity solution can be found to any desired accuracy provided the penalty constant, K , is large enough. Numerical procedures used to find the velocity solution impose some restrictions on the choice of K in the penalty formulation. The accuracy of the numerical solution can be increased by increasing K . But with a very large K , the stiffness matrix becomes ill-conditioned and the velocity solution fails to converge. This is also influenced by the machine precision and the error tolerance specified on the velocity solution. The geometry is updated after/during the velocity solution procedure. The updating process involves some error due to the truncation error of the updating method.

Thus, two sources of error that lead to volume change during simulation are the error in the velocity solution and the error of the updating scheme. The two errors should be compatible, i.e., they should be of the same order. This will optimize the number of function evaluation required to find the velocity solution and result in the least volume change. In short, an optimum value of K has to be selected to assure convergence of velocity solution and to effectively impose the incompressibility constraint.

Numerical studies show that the norm of the volumetric strain-rate is inversely proportional to the penalty constant. To avoid nonuniform deformation and strain-hardening effects, volumetric strain-rate is examined at $t = 0$. To neglect the effects of friction, $m = 0$ was used; with die-velocity of 25.4 mm/s (1 in./s) and time-increment $\Delta t = 0.01$. The following equation was used in calculating the flow stress during the simulation.

$$\bar{\sigma} = 21,936 (\bar{\epsilon})^{0.245} \text{ psi} = 151.25 (\bar{\epsilon})^{0.245} \text{ MPa} \quad (3.35)$$

Using these parameters in SPID, simulation result was obtained for cylinder upsetting experiment by Lee and Altan [1972] (presented in detail in Chapter IV). The result is shown in Fig. 3.6. This shows that the norm of the volumetric strain-rate decreases with penalty constant and their relation can be expressed as

$$\|\dot{\epsilon}_v\|_2 \propto \frac{1}{K} \quad (3.36)$$

where $\|\mathbf{v}\|_2$ represents the Euclidean norm of vector \mathbf{v} .

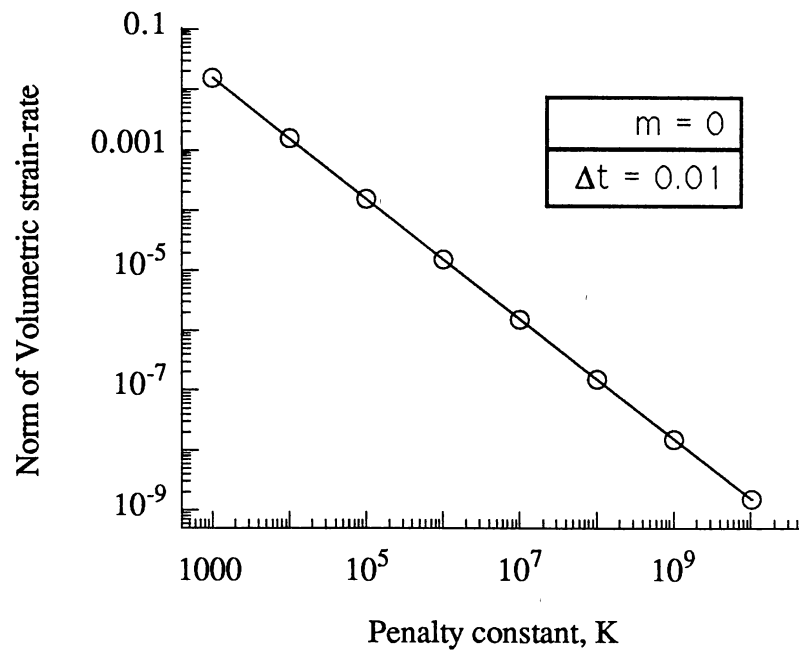


Figure 3.6 Norm of Volumetric Strain-Rate vs Penalty Constant at Time $t = 0$

Penalty Constant

Consider Euler forward method as the updating scheme and as before let Y and y denote the true and numerical solutions, respectively. Assuming $y_n = Y_n$, the error in the numerical solution can be written as

$$Y_{n+1} - y_{n+1} = h (Y'_n - y'_n) + O(h^2) \quad (3.37)$$

where h is the step size.

If $[h (Y'_n - y'_n)]$ is of the order higher than 2, then the following approximation can be made.

$$Y_{n+1} - y_{n+1} \equiv O(h^2) \quad (3.38)$$

Eqn. (3.38) implies that $Y_{n+1} - y_{n+1}$ is almost entirely due to the local truncation error inherent in the updating scheme. According to the penalty method $Y'_n - y'_n$, corresponding to the difference between the true and numerical solution, can be reduced to any desired level with a large K . Similar to Eqn. (3.36), this may be mathematically expressed as

$$Y'_n - y'_n \propto \frac{1}{K} \quad (3.39)$$

This can be rewritten as

$$Y'_n - y'_n = \frac{\mathbf{c}}{K} \quad (3.40)$$

where \mathbf{c} is a constant vector.

Eqn (3.40) can be rewritten as

$$|Y'_n - y'_n| = \frac{c}{K} \quad (3.41)$$

In vector form Eqn. (3.41) can be rewritten as

$$\|\hat{\mathbf{v}}_I - \hat{\mathbf{V}}_I\|_2 = \frac{c}{K} \quad (3.42)$$

where $\hat{\mathbf{v}}_I$ and $\hat{\mathbf{V}}_I$ are numerical and true nodal velocities, respectively, for node I, bold face implies a vector and $\|\mathbf{v}\|_2$ represents the Euclidean norm of vector \mathbf{v} .

Once again SPID was used for numerical evaluation of the constant c . Since the true solution cannot be found, the velocity solution which converges for the largest value of

K , $K = K_2$, was taken as the true solution. To neglect other factors velocity solution at time $t = 0$ is considered. The following equation was proposed to estimate the numerical value of c

$$c = \frac{\|\hat{\mathbf{v}}_I - \hat{\mathbf{V}}_I\|_2}{\left(\frac{1}{K_1} - \frac{1}{K_2}\right)} \quad (3.43)$$

where K_1 is the penalty constant used in obtaining the velocity solution $\hat{\mathbf{v}}_I$. The flow stress used is given by Eqn (3.35). The result with time increment $\Delta t = 0.01$, friction factor $m=0$, tolerance on the velocity solution of 10^{-5} , and die-velocities of 25.4 mm/s (1 in./s), 254 mm/s, and 2.54 cm/s is presented in Table 3.3. This shows that there is no significant difference in the velocity solution with increasing K beyond 1.0E6 for the simulation with a velocity of 25.4 mm/s. Thus, for this particular step an optimum value of the penalty constant is 1.0E6.

TABLE 3.3
 NUMERICAL VALUE OF C FOR DIFFERENT
 VALUES OF PENALTY CONSTANT

K_1	1.0E3	1.0E4	1.0E5	1.0E6	1.0E7
$c \left(\begin{array}{l} v = 1 \text{ in/s} \\ K_2 = 10^9 \end{array} \right)$	3.63	3.63	3.61	3.63	0.0
$c \left(\begin{array}{l} v = 1 \text{ in/s} \\ K_2 = 10^8 \end{array} \right)$	3.63	3.63	3.61	3.66	0.0
$c \left(\begin{array}{l} v = 1 \text{ in/s} \\ K_2 = 10^7 \end{array} \right)$	3.63	3.63	3.63	3.59	0.0

The tolerance ϵ is expressed as

$$\frac{\|\hat{v}_i^{(j+1)} - \hat{v}_i^{(j)}\|_2}{\|\hat{v}_i^{(j+1)}\|_2} = \frac{\|\Delta v\|_2}{\|v\|_2} \leq \epsilon \quad (3.44)$$

Since $\epsilon = 10^{-5}$, \hat{v}_i has only 5 significant decimal digits and for $K \geq 10^6$ there is no further reduction in the error Δv . Thus by increasing K beyond 1.0E6 it is not possible to attain any more significant decimal digits in the velocity solution.

Fig. 3.7 shows the volume loss (%) with reduction in height (%) for different values of K . In this case simulation for cylinder upsetting experiment was performed with $\Delta t = 0.01$, $m = 0$, die-velocity of 25.4 mm/s (1 in./sec), and the flow stress is given by Eqn. (3.35). Euler forward method is used as the updating scheme. It is observed that after a certain increase in K there is no significant decrease in the volume loss with increasing K . This is again due to the limitations posed by the machine precision being

used and the tolerance specified on the velocity solution. Thus an optimum value for K can be found which can effectively impose the condition of incompressibility. In this case an optimum value K of is $1.0E7$. This is called optimum because for $K \leq 10^7$, the error in the velocity solution is too high and the incompressibility constraint is not imposed properly, and for $K \geq 10^7$, there is no further improvement in the accuracy of the velocity solution. The floating point word lengths used [FIDAP, 1986] and the tolerance specified on the velocity solution have a strong relation to the above phenomenon.

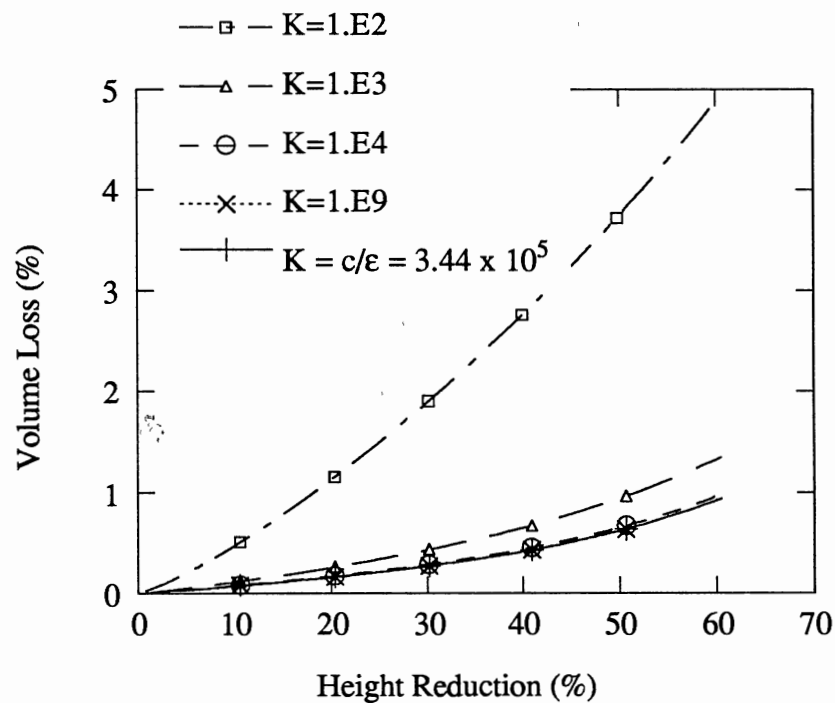


Figure 3.7 Volume Loss with Deformation for Different Values of Penalty Constant

Condition Number

A system of n linear equations can be written as $\mathbf{A} \mathbf{x} = \mathbf{b}$, where \mathbf{A} is a real or complex square matrix of order n and \mathbf{x} and \mathbf{b} are vectors of size n . In the current study \mathbf{A} is the stiffness matrix, which is banded symmetric, \mathbf{b} is the load vector, and \mathbf{x} contains the velocity vector. The condition number $\kappa(\mathbf{A})$ is a quantity which measures the sensitivity of the solution \mathbf{x} to errors in the matrix \mathbf{A} and the right side \mathbf{b} . The condition number is defined as

$$\kappa(\mathbf{A}) = \|\mathbf{A}\|_1 \|\mathbf{A}^{-1}\|_1 \quad (3.45)$$

$$\frac{\|\mathbf{x} - \bar{\mathbf{x}}\|_1}{\|\bar{\mathbf{x}}\|_1} \leq \kappa(\mathbf{A}) \frac{\|\mathbf{E}\|_1}{\|\mathbf{A}\|_1} \quad (3.46)$$

where $\|\mathbf{A}\|_1$ represents the L_1 norm of matrix \mathbf{A} , $\bar{\mathbf{x}}$ is the numerical solution and \mathbf{E} is the perturbation error in \mathbf{A} .

If the relative error in \mathbf{A} is of size ϵ , $\epsilon = \frac{\|\mathbf{E}\|_1}{\|\mathbf{A}\|_1}$, then the resulting error in \mathbf{x} can be as large as $\epsilon\kappa(\mathbf{A})$. Since it is expensive to compute the inverse of a matrix, the condition number is only estimated. Usually an estimate of the reciprocal condition number, $1/\kappa(\mathbf{A})$, is computed. If the condition number is approximately 10^d then the elements of \mathbf{x} can usually be expected to have d fewer significant figures of accuracy than the elements of \mathbf{A} . If the estimated condition number is greater than $1/\epsilon$ (where ϵ is the machine precision) then very small changes in \mathbf{A} can cause very large changes in the solution \mathbf{x} . But if the reciprocal condition number is so small that in floating point arithmetic it is negligible

compared to 1.0, then x may not have any significant figures. This condition is tested by the following logical expression.

$$(-1.0 + 1/\kappa(A)) \text{ .EQ. } 1.0 \quad (3.47)$$

If the above is true then the matrix can be considered to be singular to working precision.

An attempt was made to study the effect of K on the condition number of the stiffness matrix. The condition number was estimated using the IMSL (International Mathematical and Statistical Library) subroutine LFCRG [IMSL, 1989]. Simulation for cylinder upsetting experiment was performed with $\Delta t = 0.01$, $m = 0$, die-velocity of 25.4 mm/s (1 in./sec), and the flow stress is given by Eqn. (3.35). The result at time $t = 0$ is taken and is shown in Fig. 3.8. This was repeated with different tolerances on the velocity solution. It was found that for a constant K there is a lower limit on the tolerance that can be specified. Below this tolerance the velocity solution fails to converge. This is shown for different K in Fig. 3.9. Similarly with a constant tolerance there is upperbound on K beyond which convergence is not achieved (Fig. 3.8). Thus a proper combination of tolerance and K must be selected to ensure convergence. Fig. 3.8 shows that the condition number increases with K . It was observed that with $\epsilon = 10^{-3}$ the velocity solution at time $t = 0$ fails to converge for penalty constant larger than $1.0E10$ i.e. for $K > 10^{10}$.

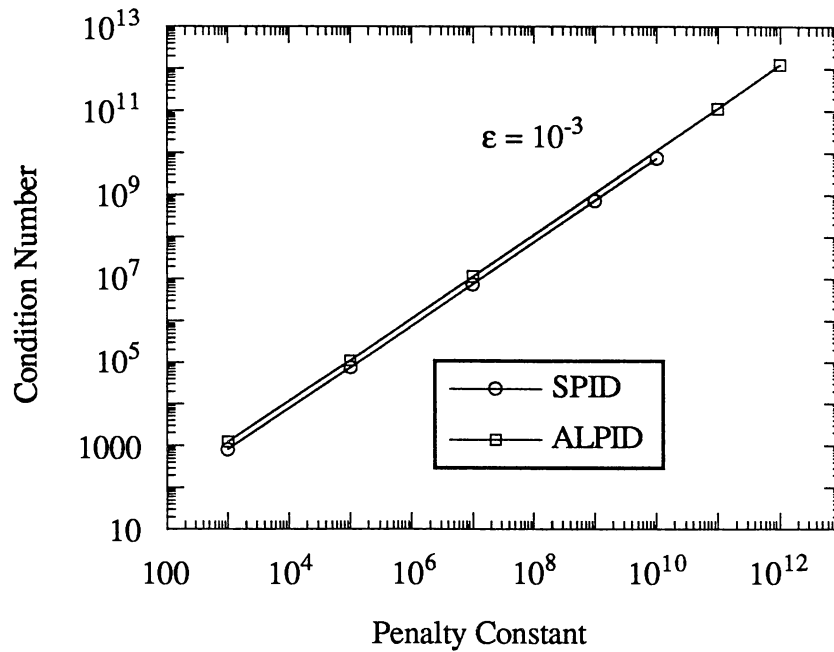


Figure 3.8 Condition Number of the Stiffness Matrix vs Penalty Constant

Example

Simulation of the cylinder upsetting experiment was done using the optimum value of K . It is assumed that the 64-bit representation of floating point numbers gives 16 significant decimal places and the condition number of the stiffness matrix is approximately 10^7 . Under the conditions assumed, the tolerance specified on the velocity solution should be greater than 10^{-7} . Euler forward method is used as the updating scheme and thereby the error in updating is $O(h^2) = 10^{-4}$. The approximation given by Eqn. (3.38) is satisfied if $h(Y' - y') \leq 10^{-5}$, i.e. $\epsilon \leq 10^{-3}$. Hence simulation was performed using $\epsilon = 10^{-5}$. The parameters used for simulation are $\Delta t = 0.01$, $m = 0$, die-velocity of 25.4 mm/s (1 in./sec),

and the flow stress is given by Eqn. (3.35). The penalty constant was evaluated using the following equation.

$$K = \frac{c}{\epsilon} = 3.44 \times 10^{-5} \quad (3.48)$$

The result is shown in Fig. 3.7 . This shows that the optimum value of K can be obtained using Eqn. (3.48) provided the choice of ϵ is proper. This value of K is quite efficient in ensuring the convergence of the velocity solution and in maintaining the volume loss within a small percentage of the deforming volume.

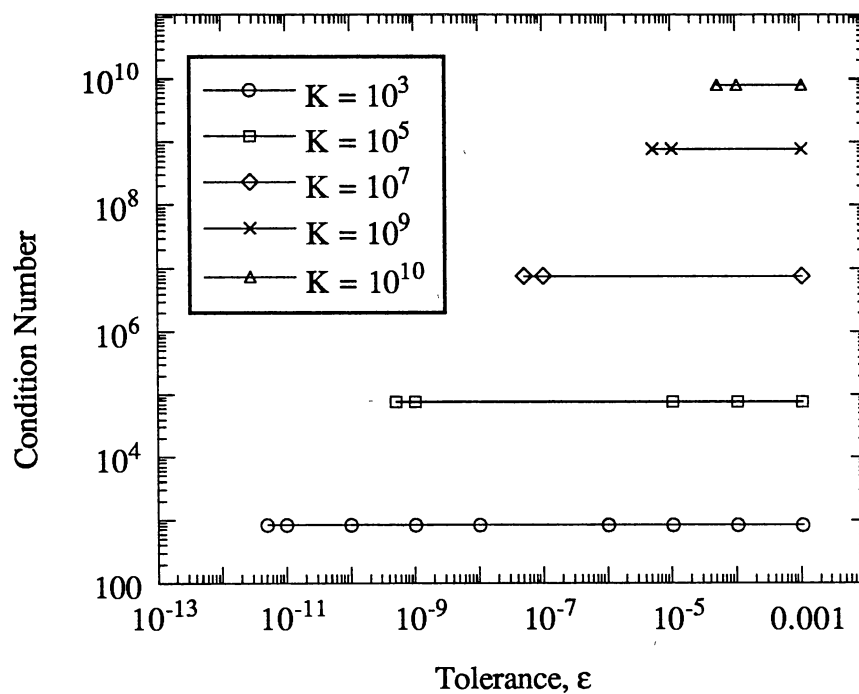


Figure 3.9 Condition Number vs Tolerance

Conclusions

Thus it can be concluded that the choice of K is influenced by several factors. The major factors that influence the choice of K are listed below.

1. In the general form the difference between the true and numerical solution can be written as

$$Y_{n+1} - y_{n+1} = \alpha h (Y'_n - y'_n) + h\tau(h) \quad (3.49)$$

where $h\tau(h)$ is the local truncation error of the updating scheme and α is a constant. The two terms on the R.H.S. should be compatible. Once the updating scheme and the step size has been selected then the order of the first term, $\alpha h (Y'_n - y'_n)$, has to be adjusted according to order of the updating method i.e. order of $[h\tau(h)]$.

2. The tolerance specified on the velocity solution determines the number of significant decimal places in the velocity solution. Thus a very large K will not yield better accuracy in the solution. Moreover with the choice of a very small tolerance velocity solution fails to converge.
3. Choice of a very large K leads to ill-condition of the resulting stiffness matrix. The stiffness matrix becomes singular and the velocity solution fails to converge.
4. For a 64-bit floating point representation there can be approximately 16 significant decimal places. The exact figure is machine dependent. It signifies the largest number α and the smallest number β on which an operation, e.g., addition can be carried out without any loss in the number of significant digits. This limits the largest K that can be used to get a convergent velocity solution.

CHAPTER IV

RESULTS AND DISCUSSION

Introduction

Validation of results obtained in simulation of axisymmetric uniform deformation process was carried out. Both the trapezoidal method and AM-2 method were implemented on a finite element based software, SPID [Kobayashi et al., 1989] (Simple Plastic Incremental Deformation). SPID uses rigid-viscoplastic material model based on the penalty constant approach. In this model the elastic effects are completely neglected. The time integration scheme used in this software for updating state variables is based on Euler forward method. The original subroutines were modified to incorporate the trapezoidal method and AM-2 method.

The following equations were used as time integration schemes for updating the geometry :

$$\hat{\mathbf{x}}_I(t_0 + \Delta t) = \hat{\mathbf{x}}_I(t_0) + \Delta t \hat{\mathbf{v}}_I(t_0) \quad (4.1)$$

$$\hat{\mathbf{x}}_I(t_0 + \Delta t) = \hat{\mathbf{x}}_I(t_0) + \frac{\Delta t}{2} [\hat{\mathbf{v}}_I(t_0 + \Delta t) + \hat{\mathbf{v}}_I(t_0)] \quad (4.2)$$

$$\hat{\mathbf{x}}_I(t_0 + \Delta t) = \hat{\mathbf{x}}_I(t_0) + \frac{\Delta t}{12} [5 \hat{\mathbf{v}}_I(t_0 + \Delta t) + 8 \hat{\mathbf{v}}_I(t_0) - \hat{\mathbf{v}}_I(t_0 - \Delta t)] \quad (4.3)$$

where $\hat{\mathbf{x}}_I(t)$ and $\hat{\mathbf{v}}_I(t)$ are nodal coordinates and nodal velocities, respectively, for element I at time t, and Δt is the time increment. Eqns. (4.1), (4.2), and (4.3) represent geometry

updating schemes based on Euler forward method, the trapezoidal method, and AM-2 method, respectively. The strain is updated in a similar manner from the strain-rate solution.

In the original program (SPID and ALPID) the geometry was updated for the next time step once the convergence of the velocity solution was achieved as shown in Fig. 4.1. Since the modified updating schemes are based on implicit methods, it was proposed to update both the geometry and the effective strain simultaneously during the solution iteration. This approach of updating the state variables during the solution iteration is shown in Fig. 4.2. It was observed that the number of iterations required to solve for the velocities did not increase significantly.

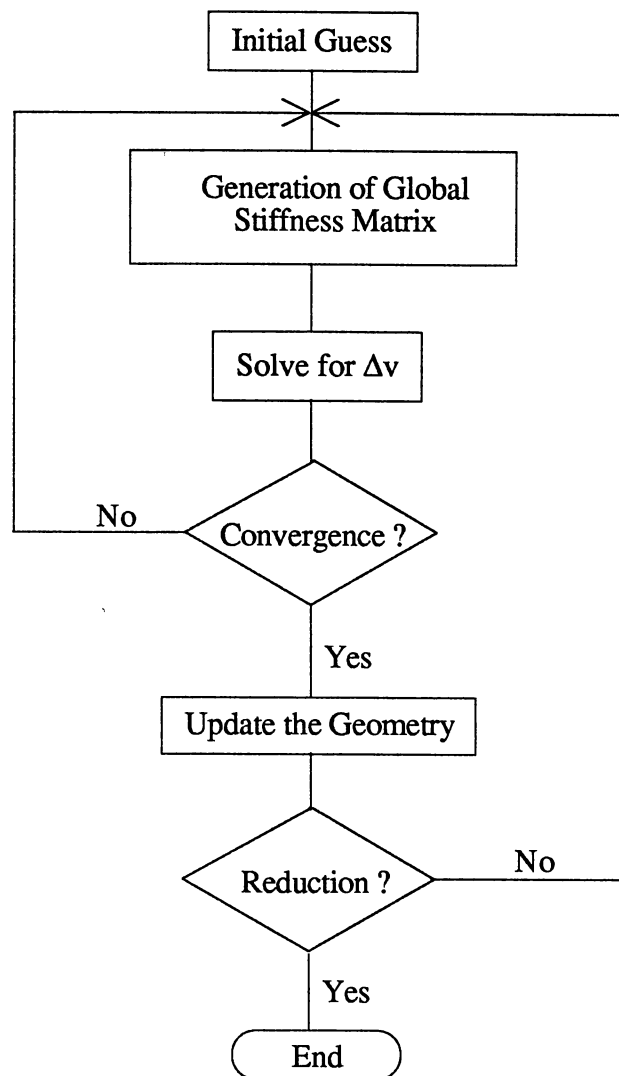


Figure 4.1 Block Diagram for Simulation Using Euler Forward Method

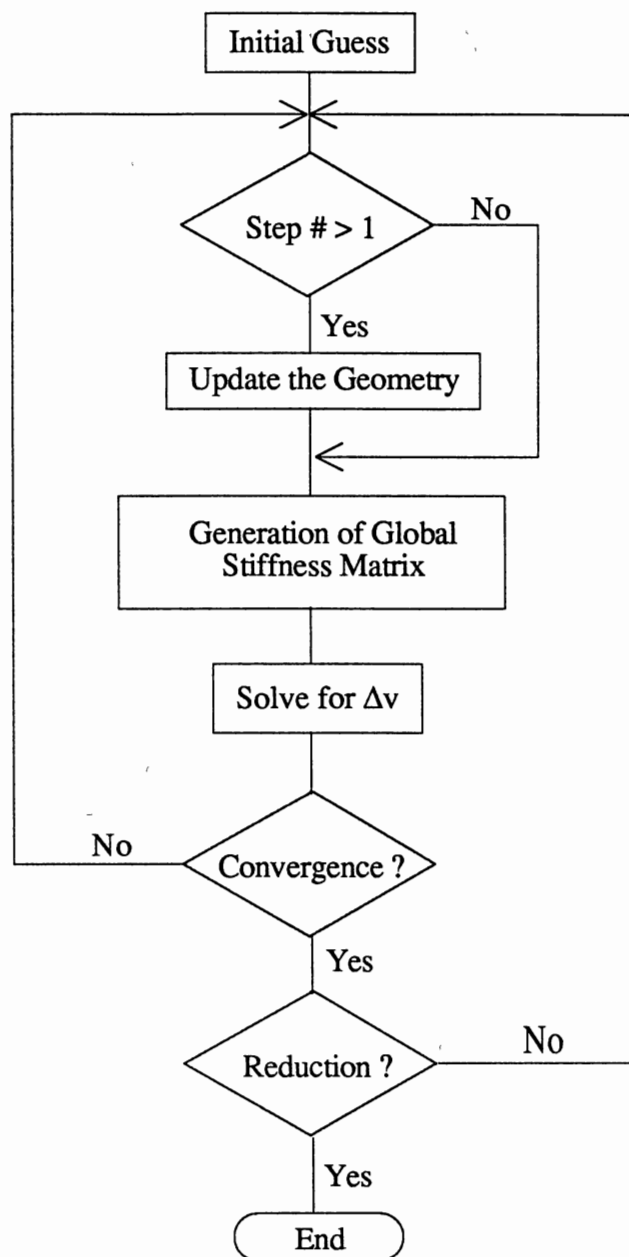


Figure 4.2 Block Diagram for Simulation Using the Trapezoidal Method

Simulation Results

Simulation of the cylinder upsetting experiments performed by Lee and Altan [1972] was carried out using both SPID and the modified versions to compare and contrast the application and the limitations of the different time integration schemes being considered in this study. Upset forging of a strain-hardening material, 1100 F aluminum alloy, was carried out at room temperature in the experiments. Cylinders with a 38.1 mm (1.5-in.) dia. \times 57.15 mm (2.25-in.) height ($H/D = 1.5$) were machined from bars that were annealed at 454.4° C (850 F) for 1.5 hr and furnace cooled. Cylinder samples were upset between hardened flat, parallel steel plates under a 889.6 kN (200,000-lb) Instron machine at 304.8 mm/s (0.2-in/min) ram speed. The magnitude of elastic deflection of the testing machine under load was 0.762 mm (0.030 in.) per 444.8 kN (100,000 lb). Consequently, the displacement measured on the testing machine was corrected in calculating strain

$\bar{\epsilon} = \ln \frac{h_0}{h_1}$, i.e. the actual height h_1 of the deformed sample had to be used in calculating $\bar{\epsilon}$.

Experiments were performed under three lubrication conditions and simulation under all the three has been carried out. The following exponential form of $\bar{\sigma}$ - $\bar{\epsilon}$ relationship [Lee and Altan, 1972] used in calculating the flow stress for simulation :

$$\bar{\sigma} = 21,936 (\bar{\epsilon})^{0.245} \text{ psi} = 151.25 (\bar{\epsilon})^{0.245} \text{ MPa} \quad (4.4)$$

Taking advantage of symmetry only a quarter was taken for simulation purpose. This is shown hatched in Fig. 4.3. This was treated as a 2-D axisymmetric problem. The initial mesh with 56 nodes and 42 elements is shown in Fig. 4.4 . Velocity boundary condition of -2.54 mm/s (-0.1 in/sec) was imposed along with friction boundary condition on the nodes touching the die. The penalty constant used during simulation was evaluated at every iteration of the nonlinear solver using the following expression

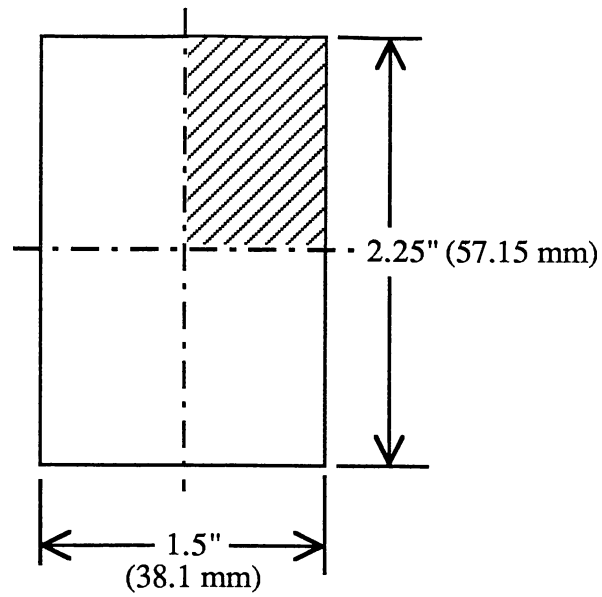


Figure 4.3 Illustration of the Quarter Taken for Simulation

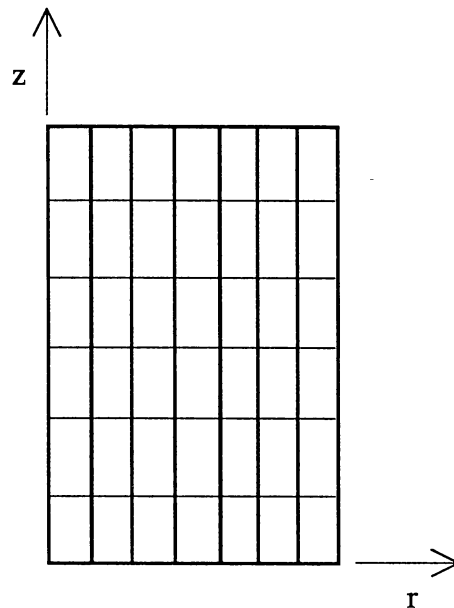


Figure 4.4 Initial Mesh Used in FE Analysis of Cylinder Upsetting
[56 Nodes and 42 Elements]

$$K = \frac{\bar{\sigma}}{\dot{\epsilon}} 1000 \quad (4.5)$$

and the tolerance specified on the velocity solution was $\epsilon = 10^{-5}$.

Results of the three lubrication conditions are :

1. Teflon. In their experiments, cylinders were upset to a total of approximately 50 percent reduction in height under uniform upsetting conditions. For this purpose, Teflon 0.254 mm (0.010-in.) thick was placed at the upper and lower interfaces after each incremental cumulative reduction of about 20, 30, 40 percent. Simulation was performed using a friction factor $m = 0.0$, time-increment $\Delta t = 0.1$, and die-velocity of 2.54 mm/s (0.1 in/sec). The load-displacement curves for 0 to 62 steps of modified programs and SPID with the same data file are given in Fig. 4.5. Experimental results corresponding to teflon lubrication condition are taken for comparison. Simulation results for all the three updating schemes agree well with experimental result. But as can be seen from Fig. 4.5, load is underpredicted by Euler forward method whereas the load values predicted by the trapezoidal and AM-2 methods are closer to the experimental values. For a reduction in height of 50 % (28.56 mm) the load predicted by Euler method is 6 % less than the experimental value, whereas, the load predicted by the two implicit methods differs by less than 3%. In this experiment bulging in upsetting of cylinders was completely eliminated and the simulation results match well with experimental result. The bulge profiles differ for different updating methods but only at a very high magnification. Hence no conclusion could be drawn from this observation and as such the associated figures are not presented.

Plots of volume change versus stroke for modified programs and SPID with the same input data file are shown in Fig. 4.6. Volume change in SPID results seem to be excessive whereas the volume change in the results of modified programs is close to zero. For a reduction in height of 50 % (1-in.), volume change in using Euler forward method is

0.7 %, whereas, volume change using the trapezoidal and AM-2 method is only 0.02%.

This shows that better results are obtained when geometry is updated using the trapezoidal method or AM-2 method than while using Euler forward method.

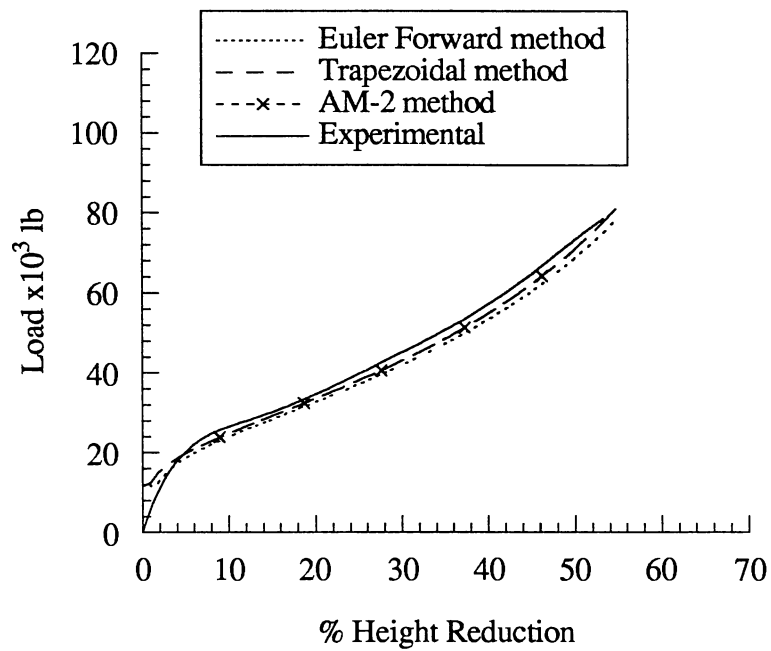


Figure 4.5 Load vs Displacement for Friction Factor of $m = 0.0$

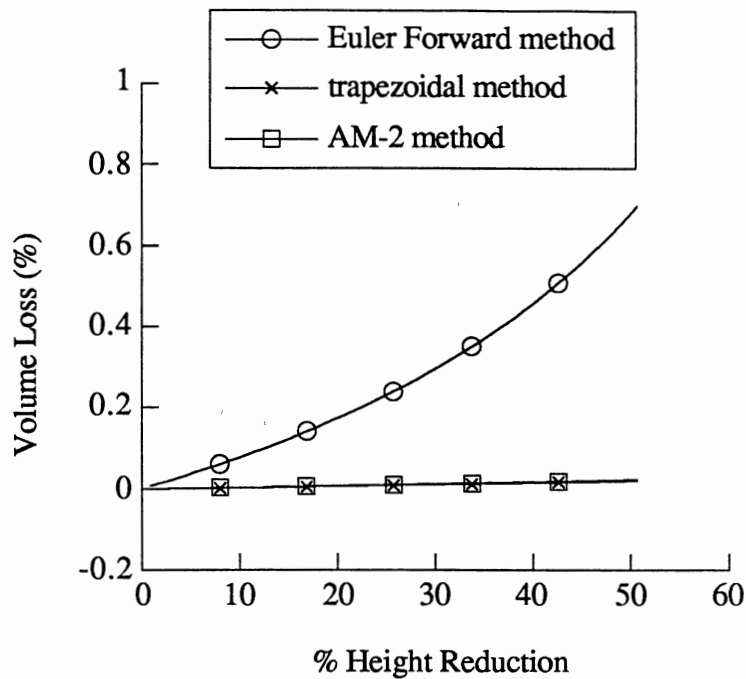


Figure 4.6 Volume Loss vs Height Reduction (%) for Friction Factor $m = 0.0$

2. Molybdenum Disulphide. In this experiment MoS_2 spray was sprayed on all surfaces of the samples and on the top and bottom dies. Simulation was performed using a friction factor $m = 0.25$. The load-displacement curves for 0 to 57 steps of modified programs and SPID with the same data file are given in Fig. 4.7. Experimental results corresponding to MoS_2 lubrication condition are taken for comparison. For a reduction in height of 50 % the load predicted by Euler forward method is 3 % less than the experimental value, whereas, the load predicted by the implicit methods differs by less than 0.5%. Plots of volume change versus stroke for modified programs and SPID with the same input data file are shown in Fig. 4.8. This shows that the volume loss in simulations by Rusia et al [1989] using ALPID is close to that given by Euler forward method using SPID. The volume loss

given by the trapezoidal and AM-2 methods is close to zero for 50 % reduction in height whereas for the same reduction it is 0.6 % for Euler forward method.

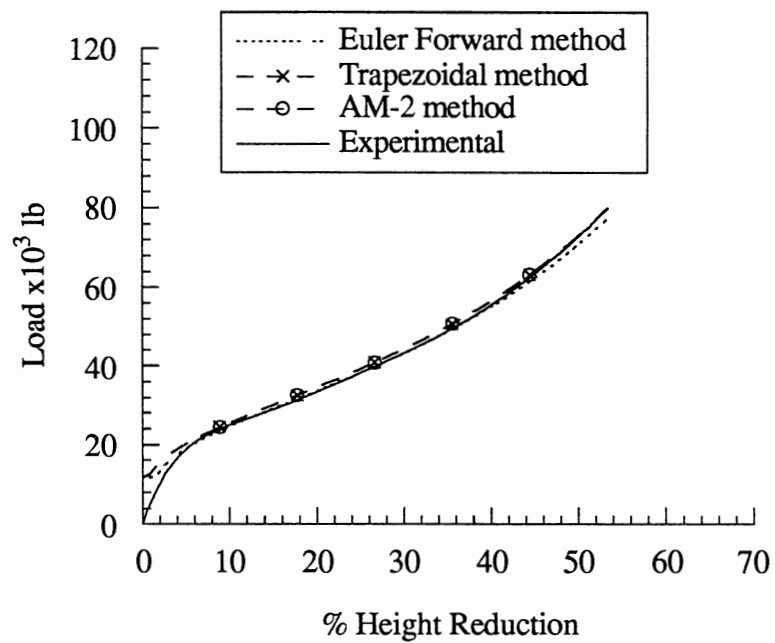


Figure 4.7 Load vs Displacement for Friction Factor of $m = 0.25$

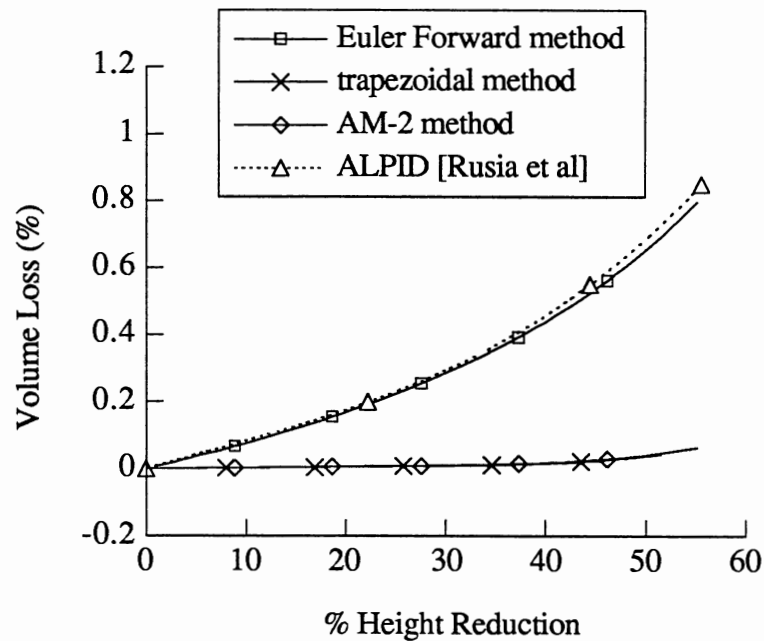


Figure 4.8 Volume Loss vs Height Reduction (%) for Friction Factor $m = 0.25$

3. Dry. In this experiment upsetting was performed for sticking friction. For this purpose, all surfaces of the samples were cleaned with acetone and dried in air. Simulation was performed with friction factor $m=1.0$. The load-displacement curves for 0 to 51 steps of modified programs and SPID with the same data file are given in Fig. 4.9. Experimental results corresponding to dry lubrication condition are taken for comparison. For a reduction in height of 45 %, the load predicted by Euler method is 5 % less than the experimental value, whereas, the load predicted by the implicit methods differs by less than 3 %.

Plots of volume change versus stroke for modified programs and SPID with the same input data file are shown in Fig. 4.10. The conclusion from these figures is same as that for the experiment with teflon-film lubrication.

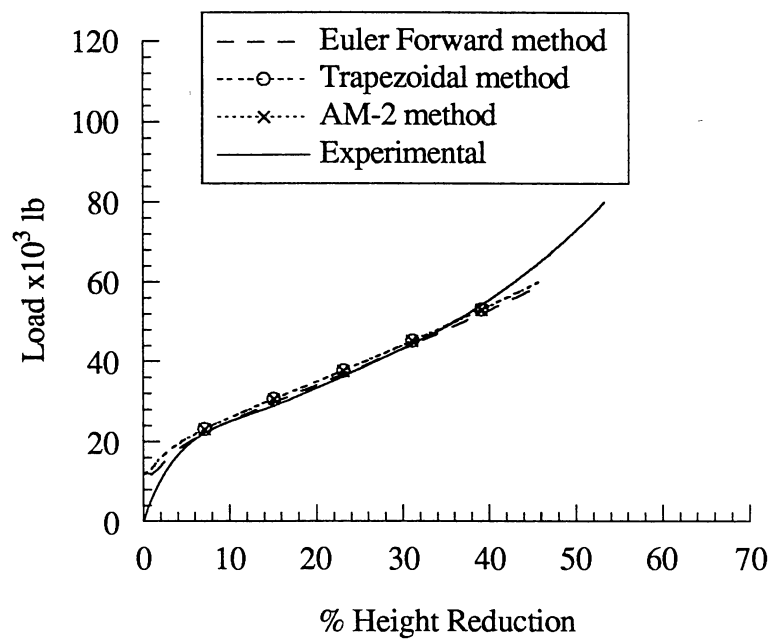


Figure 4.9 Load vs Displacement for Friction Factor of $m = 1.0$

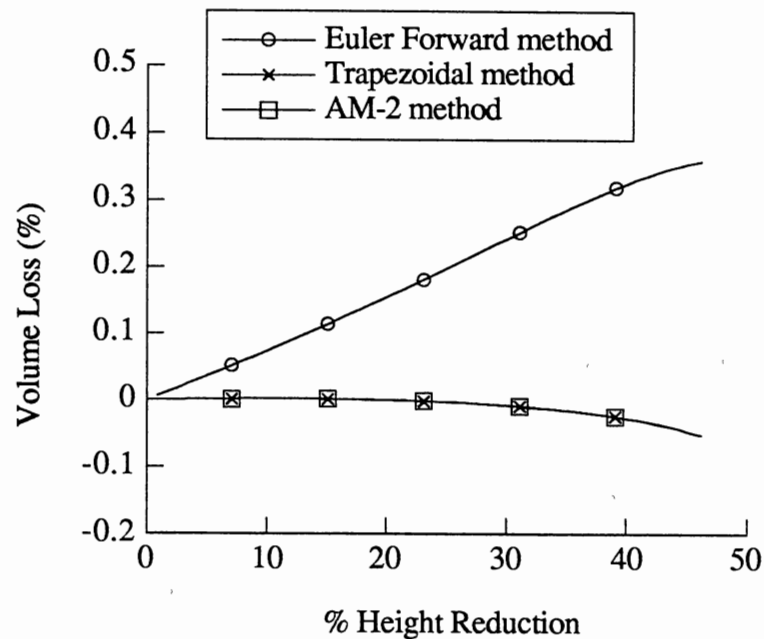


Figure 4.10 Volume Loss vs Height Reduction (%) for Friction Factor $m = 1.0$

It is observed that for all the conditions tested, both the trapezoidal and AM-2 methods yield better results compared to Euler forward method. The difference is significant for volume loss and there is an improvement in the loads predicted. It is also seen that there is no significant difference in the results between the trapezoidal and AM-2 methods. This shows that using a higher order method need not necessarily give better results and the reason behind this has been explained in Chapter III.

The trapezoidal method was implemented on ALPID 2.0 (Analysis of Large Plastic Incremental Deformation), an FE based software package for 2D simulation model. The approach used in implementing is similar to that mentioned earlier. The efficacy of the trapezoidal method as time integration scheme for other state variables was also put to test. Simulation of tapered compression experiments by Lalli [1988] was carried out in which

microhardness was updated using the trapezoidal method. Volume change with reduction in height is shown in Fig. 4.11 and load vs stroke is shown in Fig. 4.12.

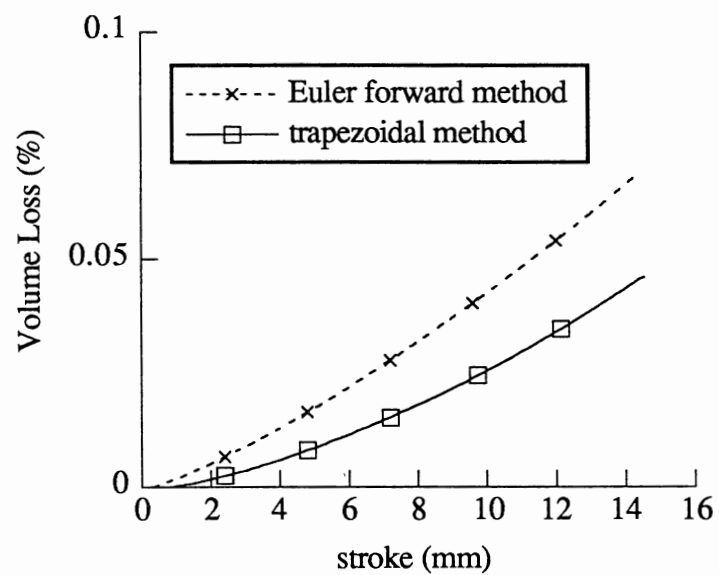


Figure 4.11 Volume Loss with Stroke (mm) Using ALPID 2.0

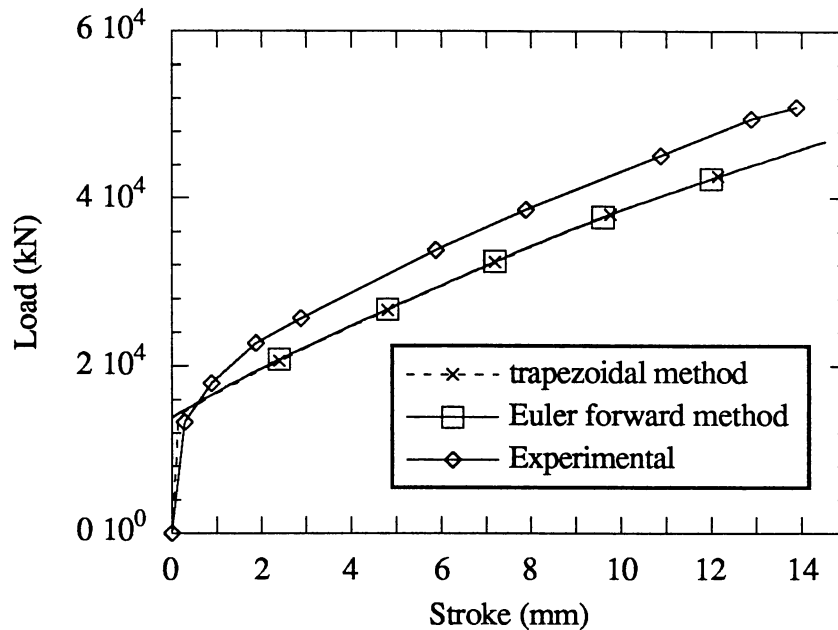


Figure 4.12 Load vs Stroke Plot Using ALPID 2.0

For comparison, simulation results [Shiau et al., 1991] using Lalli's [1988] constitutive with microhardness as an internal state variable was taken. As such simulation results were obtained using the same input data file as that used by Shiau et al [1991]. It is observed that the volume change using the trapezoidal rule is certainly less than that given by Euler forward method. There is no significant difference observed in the predicted load values. Plots of microhardness is presented in Fig. 4.13. The microhardness distribution predicted using the trapezoidal method is in close agreement with those predicted by Shiau et al. [1991] and agrees well with the experimental result.

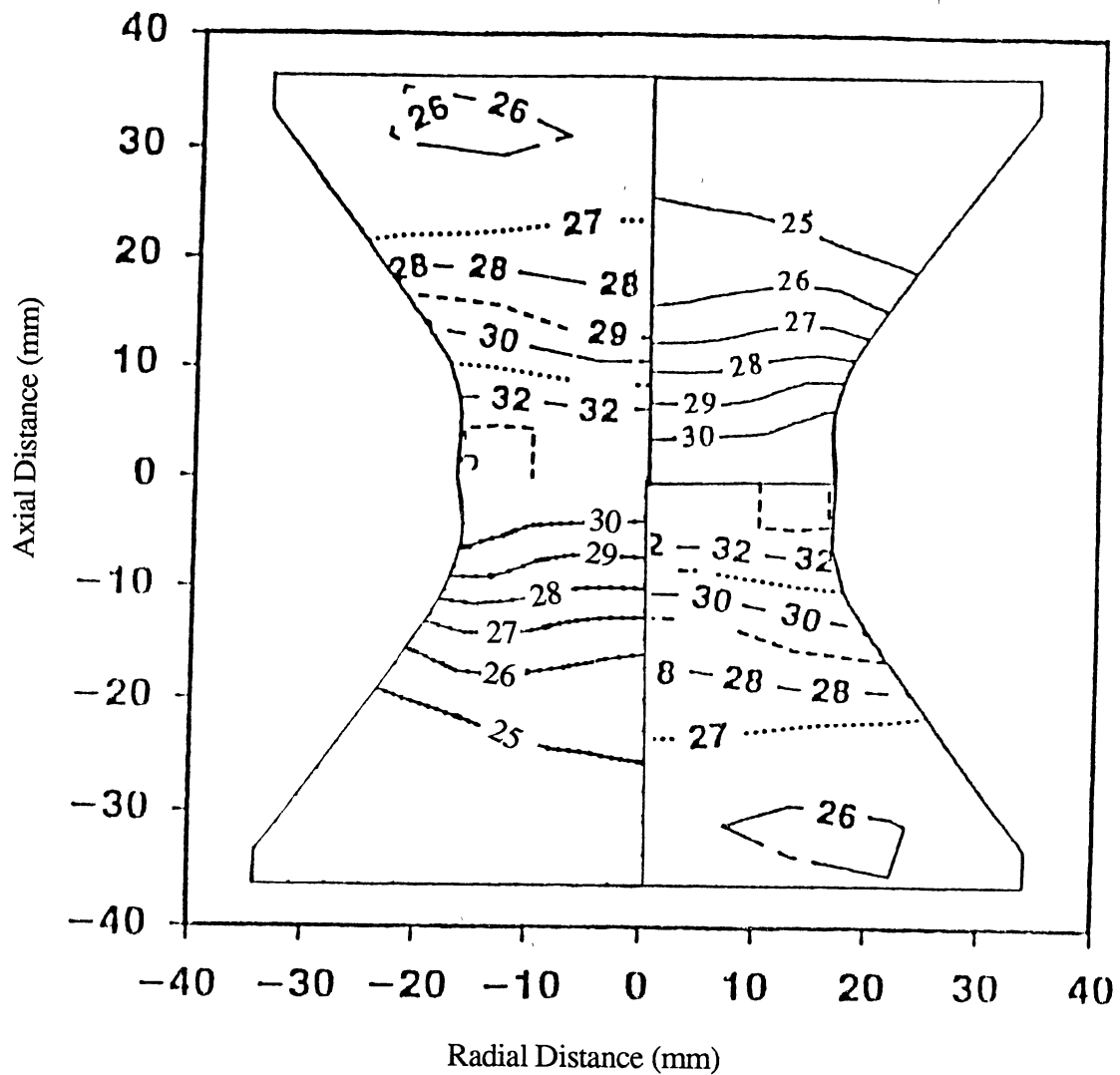


Figure 4.13 Measured Microhardness Contours, ALPID Predictions with Single Internal-State-Variable Model (Upper Right Quadrant) and ALPID Predictions Using the Trapezoidal Method for Updating Microhardness (Lower Right Quadrant) for Height Reduction of 14.48 mm at 255°C

CHAPTER V

CONCLUSIONS AND RECOMMENDATIONS

Two higher order methods were selected and successfully incorporated into well known finite element based programs, as time integration schemes for updating the state variables. The different criteria used in selection were discussed in detail. The methods selected, the trapezoidal and Adams-Moulton 2-step (AM-2) method, are implicit methods. Hence updating of the state variables (geometry, strain, etc.) was carried out during the velocity solution process. Simulation of experiments showed that the higher order methods yield better results as far as volume loss and predicted loads are concerned.

Influence of various parameters on the choice of penalty constant were studied. It was observed that the choice of K is influenced by the order of the method, step size, tolerance specified on the velocity solution, and machine precision used. A simple method has been presented to find the optimum value of penalty constant K , which is necessary to effectively impose the incompressibility condition as well as ensure convergence of the velocity solution.

Simulation results show that the trapezoidal method yields better results when compared to Euler forward method with respect to volume loss and predicted loads. The microhardness distribution obtained using the trapezoidal method compares well with the experimental data. The optimum value of K minimizes the volume loss and ensures the convergence of the velocity solution.

Further study needs to be done to quantify more precisely effects of various parameters on the choice of K . Application to other areas like fluid dynamics can be envisaged.

REFERENCES

- ALPID 2.0 (Analysis of Large Plastic Incremental Deformation for Two-Dimensional Forming), User's Manual Version 2.1, Battelle-Columbus Division, 1987.
- ALPID 3.0 (Analysis of Large Plastic Incremental Deformation for Three-Dimensional Forming), User's Manual Version 1.0, Battelle-Columbus Division, 1987.
- Altan, T., S. Oh, and H. L. Gegel, Metal Forming Fundamentals and Applications, American Society for Metals, 1983.
- Atkinson, Kendall E., An Introduction to Numerical Analysis, John Wiley and Sons, 1989.
- Bathe, Klaus-Jurgen, Finite Element Procedures in Engineering Analysis, Prentice Hall, 1982.
- Duggirala, Ravikiran , "Using the Finite Element Method in Metal-Forming Process," JOM(FEB), pp. 24-27, 1990.
- FIDAP, Users Manual, Fluid Dynamics International, Inc., 1991
- Hoff, C. and R. L. Taylor, "Higher Derivative Explicit One Step Methods for Non-linear Dynamic Problems. Part I : Design and Theory," Int. J. Num. Meth. Engng., 29, pp. 275 - 290, 1990.
- Hoff, C. and R. L. Taylor, "Higher Derivative Explicit One Step Methods for Non-linear Dynamic Problems. Part II : Practical Calculations and Comparisons with Other Methods," Int. J. Num. Meth. Engng., 29, pp. 291 - 301, 1990.
- Hosford, W. F. and R. M. Caddell, Metal Forming Mechanics and Metallurgy, Prentice Hall Inc., 1983.
- IMSL , International Mathematical and Statistical Library, User's Manual, 1987.
- Katona, Michael G., and O. C. Zienkiewicz, "A Unified Set of Single Step Algorithms Part 3: The Beta-m Method, A Generalization of The Newmark Scheme," Int. J. Num. Meth. Engng., 21, pp. 1345-1359, 1985.
- Kobayashi, S., S. I. Oh, and T. Altan, Metal Forming and the Finite-Element Method, Oxford University Press, 1989.
- Lalli, L. A., "Prediction of Hardness and Strain Distributions during Hot Deformation of Aluminium", Ph.D. Dissertation, University of Pittsburgh, 1988.

Lee, C. H. and T. Altan, "Influence of Flow Stress and Friction Upon Metal Flow in Upset Forging of Rings and Cylinders," ASME J. Engng. Indust., pp. 775 - 782, 1972.

Oden, J. T., "Penalty Method and Reduced Integration for the Analysis of Fluids," ASME AMD, pp. 21-32, 1981.

Osakada, K. , J. Nakano and K. Mori, "Finite Element Method For Rigid-Plastic Analysis of Metal Forming--Formulation for Finite Deformation," Int. J. Mech. Sci., 24 (8), pp. 459-468, 1982.

Ravi, V. P., "Steady-State Viscoplastic Analysis of Metal Flow During Cold Drawing", M. S. Thesis, Oklahoma State University, 1992.

Rusia, D. K. and J. S. Gunasekara, "A Modified Viscoplastic Formulation for Large Deformations Using Bulk Modulus," NUMIFORM, 89, pp. 587 - 592, 1989.

Sani, R. L., P. M. Gresho, R.L. Lee, D. F. Griffiths, and M. Engelman, "The Cause and Cure (?) of the Spurious Pressures Generated by Certain FEM Solutions of the Incompressible Navier-Stokes Equations : Part 1," Int. J. Num. Meth. Fluids, 1, pp. 17-43, 1981.

Shiau, Y. C., C. K. Fong, and V. P. Ravi, "Rigid Viscoplastic Tapered Compression with Microhardness as an Internal State Variable," Trans. NAMRI/SME, pp. 23-28, 1991.

Thomas, R. M. and I. Gladwell, "Variable-Order Variable-Step Algorithms for Second-Order Systems. Part 1 : The Methods," Int. J. Num. Meth. Engng., 26, pp. 39-65, 1988.

Zienkiewicz, O. C., and P. N. Godbole, "Flow of Plastic and Viscoplastic Solids With Special Reference to Extrusion and Forming Process," Int. J. Num. Meth. Engng., 8 pp. 3-16, 1974.

Zienkiewicz, O. C., W. L. Wood, N. W. Hine, and R. L. Taylor, "A Unified Set of Single Step Algorithms Part I : General Formulation and Applications," Int. J. Num. Meth. Engng., 20, pp. 1529-1552, 1984.

APPENDICES

APPENDIX A

ROUTINES FOR VOLUME CALCULATION FOR AXISYMMETRIC
UNIFORM DEFORMATION PROCESS USING
EULER FORWARD METHOD AND
TRAPEZOIDAL METHOD

```

C      TRAPEZ RULE VS EULER FORWARD METHOD ( UPDATING )
C      VOL BY UPDATING THE GEOMETRY AND ERROR FORMULA
C      TIME-INCREMENT IS CONSTANT

      IMPLICIT INTEGER*4 (I-N), REAL*8 (A-H, O-Z)
      DATA HDOT/-1.0/, DT/.01/, ERROR/1.E-8/
      DATA PI/3.1415926535898D0/
      DATA ROE/1.0/, ROI/1.0/, HO/1.0/

      MSSG = 6
      OPEN(MSSG,FILE='an1.01',STATUS='UNKNOWN',FORM='FORMATTED')
C** VOL IS THE INITIAL VOLUME

      VOL = PI * ROE*ROE*HO
      DH = DT* HDOT
      DH2 = DH*DH
      DH3 = DH**3.0
      VLNE = 0.0
      VLNI = 0.0

      DO 100 I = 1,100
        H1 = HO + DH
        ROEDOT = -0.5 * ROE * HDOT / HO
        R1E = ROE + DT * ROEDOT
        DVOLE = PI * R1E*R1E*H1
        PDVOLE = -(DVOLE-VOL)/VOL*100.0

        VLNE = VLNE + (-0.75 * DH2)/(HO*HO) * PI * ROE *ROE * HO
        PVLNE = -VLNE/VOL *100.0

        ROIDOT = -0.5 * ROI * HDOT /HO
        RIT = ROI

        DO 50 J =1,100
          R1DOT = -0.5 * RIT * HDOT / H1
          R1I = ROI + 0.5 * DT * ( R1DOT + ROIDOT )
          CHK = ABS((RIT-R1I)/R1I)
          IF(CHK .LT. ERROR) GO TO 80
          RIT = R1I
50      CONTINUE
80      CONTINUE
          R1I = RIT
          DVOLI = PI * R1I*R1I*H1
          PDVOLI = -(DVOLI-VOL) /VOL *100.0
          VLNI = VLNI + (-5./16.) * ( DH3/(HO*HO*HO))*PI*ROI*ROI*HO
          PVLNI = -VLNI/VOL *100.0
          PHT = (1.0 - H1 ) *100.0
          WRITE(MSSG,1000) PHT, PDVOLE ,PDVOLI,PVLNE,PVLNI
1000  FORMAT(f6.2,4(' ',2x,f15.7))
          IF(H1 .LT. 0.2) GO TO 110
          HO = H1
          ROE = R1E
          ROI = R1I
100  CONTINUE
110  CONTINUE
      STOP
      END

```

APPENDIX B

**ROUTINES FOR VOLUME CALCULATION FOR AXISYMMETRIC
UNIFORM DEFORMATION PROCESS
USING AM-2 METHOD**

```

C      TIME-INCREMENT IS A CONSTANT

      IMPLICIT INTEGER*4 (I-N), REAL*8 (A-H, O-Z)
      DATA HDOT/-1.0/, DT/.05/, ERROR/1.E-8/
C      DATA PI/3.1415926535898D0/
      DATA RO/1.0/, HO/1.0/

      MSSG = 18
      ibug = 10
      OPEN(MSSG, FILE='adam.05', STATUS='UNKNOWN', FORM='FORMATTED')
      OPEN(ibug, FILE='buggy', STATUS='UNKNOWN', FORM='FORMATTED')

      PI = 4.0*datan(1.d0)
C      write(*,*) pi
      VOL = PI * RO*RO*HO
      DH = DT* HDOT
      DH3 = DH**3.0
      DH4 = DH**4.0
      VLNI = 0.0

      H1 = HO + DH
      RODOT = -0.5 * RO * HDOT /HO
      RIT = RO

      DO 50 J =1,1000
      R1DOT = -0.5 * RIT * HDOT / H1
      R1 = RO + 0.5 * DT * ( R1DOT + RODOT )
      CHK = ABS((RIT-R1)/R1)
      IF(CHK .LT. ERROR) GO TO 80
      RIT = R1
50     CONTINUE

      80     CONTINUE
      VLNI = VLNI + (-5./16.) * ( DH3/(HO*HO*HO))*PI*RO*RO*HO
C      write(*,*) r1

      R1DOT = -0.5 * R1 * HDOT / H1

      DO 150 i = 1, 100
      H2 = H1 + DH
      RT = R1

      do 65 j = 1, 100
      r2dot = -0.5 * rt * hdot / h2
C      write(ibug,*) r2
      r2 = r1 + (DT/12.) * (5.0 * r2dot + 8.0 * r1dot - rodot)
      chk = abs((rt-r2)/r2)
      IF(CHK.LT.ERROR) GOTO 86
      rt = r2
65     continue

      86     CONTINUE
C      write(*,*) 'j=',j
      write(ibug,*) h2,r2
      r2dot = -0.5 * r2 * hdot / h2
      DVOLI = PI * R2*R2*H2
      PDVOLI = ((vol-DVOLI) / VOL) * 100.0

```

```
VLNI = VLNI + (35./64.)* (DH4/(Ho**4.0))* (pi*ro*ro*ho)
PVLNI = -(VLNI/vol) * 100.0

PHT = (1.0 - H2 ) * 100.0
WRITE(MSSG,1200) PHT,PDVOLI,PVLNI

IF(H2 .LT. 0.2) GO TO 211

rodot= rldot
rldot = r2dot
ro = r1
r1 = r2
ho = h1
h1 = h2

150  continue
211  continue
1200 FORMAT(f6.2,4(' ',2x,f15.9))

STOP
END
```

VITA

Rameshkumar Sivaraman

Candidate for the Degree of

Master of Science

Thesis : INVESTIGATION OF TIME INTEGRATION SCHEMES FOR FINITE
ELEMENT ANALYSIS OF METAL FORMING PROCESSES

Major Field : Mechanical Engineering

Biographical :

Personal Data : Born in India, February 13, 1970, the son of T.V.Sivaraman and Sarojini Sivaraman.

Education : Graduated from St.Xavier's College, Ranchi, India, in August 1986; received Bachelor of Technology in Mechanical Engineering from Indian Institute of Technology, Madras, India, in August 1990; completed requirements for the Master of Science degree at Oklahoma State University in December, 1992.

Professional Experience : Teaching Assistant, Department of Mechanical and Aerospace Engineering, Oklahoma State University, January, 1991, to May, 1992; Research Assistant, Department of Mechanical and Aerospace Engineering, April, 1991, to August, 1991; Project Associate, Department of Mechanical Engineering, Indian Institute of Technology, Madras, India, October, 1990, to December, 1990.